

On the IR/UV flavour connection in non-universal axion models

Luca Di Luzio, Alfredo Walter Mario Guerrero,
Xavier Ponce Díaz, Stefano Rigolin

*Istituto Nazionale di Fisica Nucleare (INFN), Sezione di Padova,
Via F. Marzolo 8, 35131 Padova, Italy*

*Dipartimento di Fisica e Astronomia ‘G. Galilei’, Università di Padova,
Via F. Marzolo 8, 35131 Padova, Italy*

Non-universal axion models, with the Peccei-Quinn (PQ) symmetry acting on Standard Model (SM) fermions in a generation-dependent way, are typically accompanied by two different sources of flavour violation, dubbed here as infrared (IR) and ultraviolet (UV). The former is due to the flavour violating axion couplings to SM fermions, while the latter arises from the heavy degrees of freedom that UV complete the axion effective field theory. We point out that these two sources of flavour violation are directly related and exemplify this connection in a general class of non-universal axion model, based on a renormalizable DFSZ-like setup with two Higgs doublets (PQ-2HDM). We next discuss the interplay of axion flavour phenomenology with the signatures stemming from the heavy radial modes of the PQ-2HDM, including meson oscillation observables and charged lepton flavour violating decays. We emphasize the strong complementarity between flavour observables, LHC direct searches and standard axion physics.

Contents

1	Introduction	2
2	Non-universal DFSZ axion models	3
2.1	Flavour violation from the light axion field (IR source)	4
2.2	Flavour violation from the heavy radial modes (UV source)	5
2.3	Connection between IR/UV sources of flavour violation	6
2.4	Non-universal PQ-2HDM Yukawa textures	7
3	Flavour phenomenology	8
3.1	LHC bounds on the 2HDM	9
3.2	Flavour constraints on the non-universal 2HDM	10
3.3	IR/UV quark flavour connection	11
3.4	IR/UV lepton flavour connection	15
4	Conclusions	17
A	PQ-2HDM scalar potential	18
B	4-fermion operators	20

C Meson mixing bounds	22
D Model-dependent bounds on the PQ-2HDM	24
E Lepton flavour violating observables	26

1 Introduction

The Peccei-Quinn (PQ) solution to the strong CP problem [1, 2] has emerged as a well-motivated paradigm beyond the Standard Model (SM), by delivering in the low-energy effective field theory (EFT) the axion field [3, 4] which also provides a natural dark matter candidate [5–7]. Invisible axion models can be classified in two broad categories, known conventionally as DFSZ [8, 9] and KSVZ [10, 11] models, depending on whether the SM fermions are charged or not under the $U(1)_{\text{PQ}}$ symmetry. In the former case, only the scalar sector of the SM is extended, by a second Higgs doublet and a SM singlet that allows to establish the hierarchy between the PQ and electroweak breaking scales. In the original formulation of the DFSZ model [8, 9] the SM fermions PQ-charge assignment is flavour blind, namely SM fermions with the same hypercharge share also the same PQ charge. On the other hand, non-universal variants of the DFSZ model (and in particular of the original WW axion model [3, 4]), in which the PQ symmetry acts on SM fermions in a generation-dependent way, appeared in the late 80’s [12–14], in the effort to explain in terms of a heavy axion the anomalous observation of a narrow e^+e^- pair peak at 1.8 MeV in heavy ion collision at the GSI [15, 16].

From a modern perspective, non-universal axion models can be motivated in several respects: *i*) their potential connection to the SM flavour puzzle, namely explaining the observed pattern of SM fermion masses and mixings in terms of a non-universal $U(1)_{\text{PQ}}$ acting as a flavour symmetry (see e.g. [17–20]); *ii*) the possibility of suppressing the axion couplings to nucleons and electrons, leading to the so-called “astrophobic” axion scenario [21] (see also [22–26]), which allows to relax astrophysical bounds on the axion decay constant; *iii*) the experimental opportunity of discovering the axion via flavoured axion searches (see e.g. [27–34]), which offer a complementary probe with respect to standard axion detection strategies [35, 36].

One of the most striking consequences of non-universal axion models is that, after going to the mass basis, fermion rotation matrices beyond the CKM/PMNS combinations become physical and thus can be probed via flavour violating axion couplings to SM fermions. We will indicate this type of flavour violation as of low-energy or infrared (IR) type, in the sense that it stems from the light axion field. However, this is not the only flavour violation to be expected, since the ultraviolet (UV) completion of the axion EFT might leave behind extra sources of flavour violation, indicated in the following as of high-energy or UV type. While we expect this to be a generic feature of axion EFTs, the scope of the present paper is to exemplify this connection in a general class of renormalizable (i.e. fully calculable) non-universal DFSZ-like models, whose scalar sector is based on a SM singlet and two Higgs doublets which couple non-universally to different generations of up- and down-type quarks (and charged leptons). Since the SM fermion mass matrices and the Yukawa interactions of the two Higgs doublet model (2HDM) are non-simultaneously diagonalizable, new flavour violating UV sources arise from the Yukawa couplings of the 2HDM degrees of freedom. Note that the mass scale of the non-SM-like Higgs scalars is a free parameter, ranging from a few hundreds of GeV (experimentally bounded by LHC direct searches) up to the PQ breaking scale, of the order of the axion decay constant, f_a . In this paper, we will entertain the bottom-up perspective that the 2HDM is not completely decoupled from the TeV scale,¹ and thus its degrees of freedom can be directly

¹A low-scale 2HDM within a PQ setup is theoretically motivated by the possibility of establishing the hierarchy between the electroweak and PQ scales in a “technically natural way”, i.e. stable under radiative corrections thanks to the presence of “ultra-weak” couplings in the scalar potential (see Appendix A for further details).

tested at the LHC and indirectly via flavour violating processes.

The aim of this paper, is to underline the general correlation between IR and UV sources of flavour violation in non-universal DFSZ-like axion models, focusing on flavour violating observables both in the quark and lepton sector.² In particular, we will show that the pattern of flavour violation involving the light axion field is directly correlated to that of the heavy radial modes of the 2HDM. Assuming for instance a QCD axion discovery in a golden channel like e.g. $K \rightarrow \pi a$ (which would definitely point to a tree-level source of flavour violation in s - d axion couplings), allows us to predict a definite pattern of flavour violation from the 2HDM heavy scalars in s - d transitions, e.g. in K^0 - \bar{K}^0 mixing. The bound arising from the latter observable can be then confronted with LHC direct searches, as well as with astrophysical bounds on the axion decay constant. Similar considerations apply also to other phenomenologically relevant quark flavour transitions involving B and D mesons or to lepton flavour violating (LFV) decays.

The paper is structured as follows. Section 2 focuses on theoretical aspects of the IR/UV flavour connection. We first introduce a general class of non-universal axion models (the only assumption being here a minimal field content and renormalizability) and recall the pattern of flavour violating axion couplings in terms of PQ charges. Next, we discuss the structure of a general flavour non-conserving 2HDM in the presence of a $U(1)_{\text{PQ}}$ symmetry (hereby denoted as PQ-2HDM), and work out the flavour violating couplings of the 2HDM scalar fields and the associated 4-fermion operators that are generated after integrating out the heavy radial modes. A simplified class of non-universal axion models is also introduced, in order to have an explicit realization as a benchmark scenario. Phenomenological aspects, including LHC bounds and flavour constraints on the non-universal 2HDM are discussed in Section 3, together with the aforementioned interplay between flavoured axion searches and other more standard flavour violating processes, both in the hadronic and leptonic sectors. We summarize our conclusions in Section 4, while more technical details about the scalar potential and flavour violating observables are deferred to Appendices A–E.

2 Non-universal DFSZ axion models

The scalar sector of the DFSZ model includes two Higgs doublets $H_{1,2} \sim (1, 2, -1/2)$ endowed with PQ charges $\mathcal{X}_{1,2}$ and an extra complex SM-singlet $\phi \sim (1, 1, 0)$, with PQ charge \mathcal{X}_ϕ , needed for decoupling the PQ and electroweak breaking scales. Singlet and doublet scalar fields are coupled via a single non-hermitian operator, $H_2^\dagger H_1 \phi$, thus implying $\mathcal{X}_2 - \mathcal{X}_1 = \mathcal{X}_\phi = 1$, by normalizing to 1 the PQ charge of the singlet.³ In the following, we will also require the orthogonality of the PQ and hypercharge currents (see e.g. [38]), thus ensuring the absence of a mixed $Z^\mu \partial_\mu a$ kinetic term. This fixes the PQ charges of the two Higgs doublets as $\mathcal{X}_1 = -s_\beta^2 \equiv -\sin^2 \beta$ and $\mathcal{X}_2 = c_\beta^2 \equiv \cos^2 \beta$, in terms of the vacuum angle, $t_\beta \equiv \tan \beta = v_2/v_1$, where $v_{1,2}$ are the $H_{1,2}$ vacuum expectation values (VEVs) with $v^2 = v_1^2 + v_2^2 \simeq (246 \text{ GeV})^2$. Other details concerning the renormalizable DFSZ scalar potential, the implementation of the hierarchy between the PQ and the electroweak scales and the resulting scalar spectrum are deferred to Appendix A.

The Yukawa sector of the 2HDM in the presence of a $U(1)_{\text{PQ}}$ symmetry can be written in a compact form as

$$\begin{aligned} \mathcal{L}_Y^{\text{PQ-2HDM}} = & -\bar{q}_L(Y_1^u H_1 + Y_2^u H_2)u_R + \bar{q}_L(Y_1^d \tilde{H}_1 + Y_2^d \tilde{H}_2)d_R \\ & + \bar{\ell}_L(Y_1^e \tilde{H}_1 + Y_2^e \tilde{H}_2)e_R + \text{h.c.}, \end{aligned} \quad (2.1)$$

²For a related work focusing on flavour violation in the charged-lepton sector, see Ref. [37].

³Other choices, e.g. $H_2^\dagger H_1 \phi^2$ as in the original DFSZ model [8, 9], are possible as well at the renormalizable level. The general conclusions of this paper do not depend on this particular choice, which affects instead the periodicity of the axion potential via the so-called domain-wall number (see e.g. [38]).

where $\tilde{H}_{1,2} = (i\sigma^2)H_{1,2}^*$ and $Y_{1,2}^f$ are generic three-dimensional matrices. We do not specify the origin of neutrino masses, the effects of which will be neglected in the present discussion. Requiring the $U(1)_{\text{PQ}}$ invariance on the Yukawa Lagrangian implies the following sum rules in flavour space:

$$-\mathcal{X}_q Y_{1,2}^u + Y_{1,2}^u \mathcal{X}_u + \mathcal{X}_{1,2} Y_{1,2}^u = 0, \quad (2.2)$$

$$-\mathcal{X}_q Y_{1,2}^d + Y_{1,2}^d \mathcal{X}_d - \mathcal{X}_{1,2} Y_{1,2}^d = 0, \quad (2.3)$$

$$-\mathcal{X}_\ell Y_{1,2}^e + Y_{1,2}^e \mathcal{X}_e - \mathcal{X}_{1,2} Y_{1,2}^e = 0, \quad (2.4)$$

where the left ($\mathcal{X}_{q,\ell}$) and right ($\mathcal{X}_{u,d,e}$) SM fermion PQ charges are diagonal, but in general not universal, three-dimensional matrices. Note that the PQ symmetry requires some of the Yukawa entries to vanish. For instance, in the universal DFSZ framework [8, 9] one imposes $Y_1^u = Y_2^{d,e} = 0$, falling into a type-II 2HDM scenario. In Section 2.4 we will provide two explicit examples of non-universal PQ-2HDM Yukawa textures.

2.1 Flavour violation from the light axion field (IR source)

The low-energy axion field, which spans over the neutral angular modes of the scalar multiplets

$$\phi \supset \frac{v_\phi}{\sqrt{2}} e^{ia_\phi/v_\phi}, \quad H_1 \supset \frac{v_1}{\sqrt{2}} e^{ia_1/v_1} \begin{pmatrix} 1 \\ 0 \end{pmatrix}, \quad H_2 \supset \frac{v_2}{\sqrt{2}} e^{ia_2/v_2} \begin{pmatrix} 1 \\ 0 \end{pmatrix}, \quad (2.5)$$

is defined as [38]

$$a = \frac{1}{v_{\text{PQ}}} \left(v_\phi a_\phi + v(-s_\beta^2 c_\beta a_1 + c_\beta^2 s_\beta a_2) \right) \simeq a_\phi, \quad v_{\text{PQ}}^2 = v_\phi^2 + v^2 c_\beta^2 s_\beta^2 \simeq v_\phi^2, \quad (2.6)$$

where the \simeq relation holds once $v_\phi \gg v$ is imposed. The axion effective Lagrangian below the electroweak scale reads [38]

$$\mathcal{L}_a \supset \frac{g_s^2}{32\pi^2} \frac{a}{f_a} G\tilde{G} + \frac{E}{N} \frac{e^2}{32\pi^2} \frac{a}{f_a} F\tilde{F} + \sum_{f=u,d,e} \frac{\partial_\mu a}{2f_a} \bar{f}_i \gamma^\mu \left((C_f^V)_{ij} + (C_f^A)_{ij} \gamma_5 \right) f_j, \quad (2.7)$$

where E/N is the ratio between the electromagnetic and QCD anomaly of the PQ current (for typical values in concrete axion models, see e.g. [39, 40]), and the axion decay constant is defined by $f_a = v_{\text{PQ}}/(2N)$. The axion vector and axial couplings to fermions can be written as

$$C_f^{V,A} = C_f^R \pm C_f^L, \quad C_f^{R,L} = \frac{1}{2N} V_{f_{R,L}}^\dagger \mathcal{X}_{f_{R,L}} V_{f_{R,L}} \quad (f = u, d, e), \quad (2.8)$$

in terms of the PQ charges $\mathcal{X}_{f_{L,R}}$ and of the unitary matrices, $V_{f_{L,R}}$, which diagonalize the SM fermion mass terms:

$$\hat{M}_f \equiv V_{f_L}^\dagger M_f V_{f_R}. \quad (2.9)$$

Therefore, the $C_f^{V,A}$ parameters encode all the IR sources of flavour violation, stemming from the light axion field. In the present work we will neglect renormalization group corrections on the $C_f^{V,A}$ couplings (see [24, 41–44]). This is a reasonable approximation under the assumption of a (at most) TeV-scale 2HDM, being running effects proportional to $\log m_H/m_t$, with m_H labelling the typical mass scale of the 2HDM radial modes in the decoupling limit (see Appendix A for a detailed discussion of the scalar spectrum).

2.2 Flavour violation from the heavy radial modes (UV source)

The SM fermion mass matrices in the PQ-2HDM follow from Eq. (2.1) after setting the Higgs fields on their VEVs, and read

$$M_u = \frac{v}{\sqrt{2}} c_\beta Y_1^u + \frac{v}{\sqrt{2}} s_\beta Y_2^u, \quad M_d = \frac{v}{\sqrt{2}} c_\beta Y_1^d + \frac{v}{\sqrt{2}} s_\beta Y_2^d, \quad M_e = \frac{v}{\sqrt{2}} c_\beta Y_1^e + \frac{v}{\sqrt{2}} s_\beta Y_2^e. \quad (2.10)$$

Since in non-universal PQ models the mass matrices and the Yukawa interactions are not simultaneously diagonalizable, flavour violating Higgs couplings to fermions are generated at tree level both in the neutral and charged sector. To derive those interactions, we first decompose the two Higgs doublets in terms of mass and charge eigenstates, comprising h (the SM-like Higgs) and H, A, H^\pm (the heavy radial modes). In the unitary gauge one has (see Appendix A)

$$H_1 = \begin{pmatrix} \frac{1}{\sqrt{2}}(c_\beta v - s_\alpha h + c_\alpha H - i s_\beta A) \\ -s_\beta H^- \end{pmatrix}, \quad H_2 = \begin{pmatrix} \frac{1}{\sqrt{2}}(s_\beta v + c_\alpha h + s_\alpha H + i c_\beta A) \\ c_\beta H^- \end{pmatrix}. \quad (2.11)$$

After unfolding the $SU(2)_L$ structure in Eq. (2.1) and projecting onto the fermion mass basis, $f_{L,R} \rightarrow V_{f_{L,R}} f_{L,R}$ (with $f = u, d, e$), we obtain the following Yukawa Lagrangian

$$\begin{aligned} \mathcal{L}_Y^{\text{PQ-2HDM}} \supset & - \sum_{f=u,d,e} \bar{f}_{Li} C_{ij}^{h_f} f_{Rj} h - \sum_{f=u,d,e} \bar{f}_{Li} C_{ij}^{H_f} f_{Rj} H - \sum_{f=u,d,e} \bar{f}_{Li} C_{ij}^{A_f} f_{Rj} A \\ & - \sqrt{2} \left(\bar{d}_{Li} V_{ik}^\dagger C_{kj}^{H_u^-} u_{Rj} H^- + \bar{u}_{Li} V_{ik} C_{kj}^{H_d^+} d_{Rj} H^+ + \bar{\nu}_{Li} U_{ik}^\dagger C_{kj}^{H_e^+} e_{Rj} H^+ \right) + \text{h.c.}, \end{aligned} \quad (2.12)$$

where the CKM and PMNS mixing matrix entering in the charged-current interactions are defined respectively as $V \equiv V_{\text{CKM}} = V_{u_L}^\dagger V_{d_L}$ and $U \equiv U_{\text{PMNS}} = V_{e_L}^\dagger V_{\nu_L}$, and the Higgs flavour violating coefficients C_{ij} read (see also [37])

$$C_{ij}^{h_u} = \frac{m_{u_i}}{v s_\beta} \delta_{ij} c_\alpha + \frac{1}{\sqrt{2}} \frac{-c_{\alpha-\beta}}{s_\beta} \epsilon_{ij}^u, \quad C_{ij}^{h_d(h_e)} = \frac{m_{d_i(e_i)}}{v c_\beta} \delta_{ij} (-s_\alpha) + \frac{1}{\sqrt{2}} \frac{c_{\alpha-\beta}}{c_\beta} \epsilon_{ij}^{d(e)}, \quad (2.13)$$

$$C_{ij}^{H_u} = \frac{m_{u_i}}{v s_\beta} \delta_{ij} s_\alpha + \frac{1}{\sqrt{2}} \frac{-s_{\alpha-\beta}}{s_\beta} \epsilon_{ij}^u, \quad C_{ij}^{H_d(H_e)} = \frac{m_{d_i(e_i)}}{v c_\beta} \delta_{ij} c_\alpha + \frac{1}{\sqrt{2}} \frac{s_{\alpha-\beta}}{c_\beta} \epsilon_{ij}^{d(e)}, \quad (2.14)$$

$$C_{ij}^{A_u} = \frac{m_{u_i}}{v s_\beta} \delta_{ij} (i c_\beta) + \frac{1}{\sqrt{2}} \frac{-i}{s_\beta} \epsilon_{ij}^u, \quad C_{ij}^{A_d(A_e)} = \frac{m_{d_i(e_i)}}{v c_\beta} \delta_{ij} (i s_\beta) + \frac{1}{\sqrt{2}} \frac{-i}{c_\beta} \epsilon_{ij}^{d(e)}, \quad (2.15)$$

$$C_{ij}^{H_u^-} = \frac{m_{u_i}}{v s_\beta} \delta_{ij} c_\beta - \frac{1}{\sqrt{2}} \frac{\epsilon_{ij}^u}{s_\beta}, \quad C_{ij}^{H_d^+(H_e^+)} = \frac{m_{d_i(e_i)}}{v c_\beta} \delta_{ij} s_\beta - \frac{1}{\sqrt{2}} \frac{\epsilon_{ij}^{d(e)}}{c_\beta}, \quad (2.16)$$

with

$$\epsilon_{ij}^u = (V_{u_L}^\dagger Y_1^u V_{u_R})_{ij}, \quad \epsilon_{ij}^d = (V_{d_L}^\dagger Y_2^d V_{d_R})_{ij}, \quad \epsilon_{ij}^e = (V_{e_L}^\dagger Y_2^e V_{e_R})_{ij}. \quad (2.17)$$

Therefore, all the neutral and charged flavour violating sources in the Higgs sector are encoded into the ϵ^f parameters. Note that, besides the heavy Higgs radial modes, also the SM-like Higgs features flavour violating couplings (cf. Eq. (2.13)). However, all the tree-level flavour changing neutral current contributions arising from the light Higgs sector decouple faster than the radial mode ones, since $c_{\alpha-\beta} \propto 1/m_H^2$ in the decoupling limit (cf. Eq. (A.28)).

To connect with typical low-energy flavour observables, like for example meson oscillations, one has to integrate out both the heavy radial modes, H, A, H^\pm and the SM-like Higgs, h , obtaining the $d = 6$ low-energy effective Lagrangian describing the (light) quarks and leptons 4-fermion interactions

$$\mathcal{L}_{\text{EFT}}^{4\text{-fermion}} = \mathcal{L}_{\text{EFT}}^{4\text{-quark}} + \mathcal{L}_{\text{EFT}}^{\text{semi-lept}} + \mathcal{L}_{\text{EFT}}^{4\text{-lept}}. \quad (2.18)$$

All the operators appearing in the 4-quark, semi-leptonic and 4-lepton sectors, together with the expressions of the corresponding Wilson coefficients as a function of the PQ-2HDM parameters are listed in Appendix B.

2.3 Connection between IR/UV sources of flavour violation

The IR sources of flavour violation, $C_{u,d,e}^{V,A}$, involving the light axion field and the UV sources, $\epsilon^{u,d,e}$, involving the heavy radial modes of the PQ-2HDM, turn out to be related thanks to Eqs. (2.2)–(2.4), which encode the action of the $U(1)_{\text{PQ}}$ symmetry on the Yukawa sector of the PQ-2HDM. By means of the SM fermion masses in Eq. (2.10) it is possible to rewrite the Yukawa matrices in terms of the (non-universal) fermionic PQ charges as

$$Y_1^u = \frac{\sqrt{2}}{vc_\beta} (-\mathcal{X}_q M_u + M_u \mathcal{X}_u + \mathcal{X}_2 M_u) , \quad Y_2^u = \frac{\sqrt{2}}{vs_\beta} (\mathcal{X}_q M_u - M_u \mathcal{X}_u - \mathcal{X}_1 M_u) , \quad (2.19)$$

$$Y_1^d = \frac{\sqrt{2}}{vc_\beta} (\mathcal{X}_q M_d - M_d \mathcal{X}_d + \mathcal{X}_2 M_d) , \quad Y_2^d = \frac{\sqrt{2}}{vs_\beta} (-\mathcal{X}_q M_d + M_d \mathcal{X}_d - \mathcal{X}_1 M_d) , \quad (2.20)$$

$$Y_1^e = \frac{\sqrt{2}}{vc_\beta} (\mathcal{X}_\ell M_e - M_e \mathcal{X}_e + \mathcal{X}_2 M_e) , \quad Y_2^e = \frac{\sqrt{2}}{vs_\beta} (-\mathcal{X}_\ell M_e + M_e \mathcal{X}_e - \mathcal{X}_1 M_e) , \quad (2.21)$$

where the PQ charge relation $\mathcal{X}_2 - \mathcal{X}_1 = 1$ arising from the scalar potential has also been used. Hence, by exploiting the definitions of $C_f^{L,R}$ and ϵ^f in Eq. (2.8) and Eq. (2.17), we can write the following expression relating the flavour violating couplings of the axion field and the heavy radial modes:

$$\epsilon^u = \frac{2N\sqrt{2}}{vc_\beta} \left(-C_u^L \hat{M}_u + \hat{M}_u C_u^R + \frac{\mathcal{X}_2}{2N} \hat{M}_d \right) , \quad (2.22)$$

$$\epsilon^d = \frac{2N\sqrt{2}}{vs_\beta} \left(-C_d^L \hat{M}_d + \hat{M}_d C_d^R - \frac{\mathcal{X}_1}{2N} \hat{M}_d \right) , \quad (2.23)$$

$$\epsilon^e = \frac{2N\sqrt{2}}{vs_\beta} \left(-C_e^L \hat{M}_e + \hat{M}_e C_e^R - \frac{\mathcal{X}_1}{2N} \hat{M}_e \right) . \quad (2.24)$$

Eqs. (2.22)–(2.24) provide the aforementioned connection between the IR and UV sources of flavour violation, and they apply to the most general class of renormalizable non-universal axion models based on two Higgs doublets. Notice that these relations do not depend explicitly on the unknown fermion mass rotation matrices, but only on the physical fermion masses and fermion couplings to the axion. Moreover, notice that the terms proportional to the Higgs doublet PQ charges, $\mathcal{X}_{1,2}$, are diagonal and hence they do not intervene in flavour violating interactions. In addition, from the hermiticity of the $C_f^{L,R}$ matrices, it follows that transposed off-diagonal entries can be simply related through

$$(\epsilon_{ji}^f)^* = \epsilon_{ij}^f (m_{f_i} \leftrightarrow m_{f_j}) . \quad (2.25)$$

For a more transparent connection with flavour observables, it is useful to rewrite Eqs. (2.22)–(2.24) in terms of vector and axial flavour violating couplings. For instance, the off-diagonal d -quark entries read:

$$(\epsilon_A^d)_{ij} \equiv \epsilon_{ij}^d + \epsilon_{ji}^{d*} = \sqrt{2} \frac{2N}{vs_\beta} (m_{d_i} + m_{d_j}) (C_d^A)_{ij} , \quad (i \neq j) \quad (2.26)$$

$$(\epsilon_V^d)_{ij} \equiv \epsilon_{ij}^d - \epsilon_{ji}^{d*} = \sqrt{2} \frac{2N}{vs_\beta} (m_{d_i} - m_{d_j}) (C_d^V)_{ij} . \quad (i \neq j) \quad (2.27)$$

The charged-lepton coefficients are simply obtained by replacing $d \rightarrow e$ in Eqs. (2.26)–(2.27), while the up-quark ones can be obtained via the substitutions $d \rightarrow u$ and $s_\beta \rightarrow c_\beta$. In addition, for describing $\Delta F = 2$ observables (cf. Eqs. (C.12)–(C.17)) the following combinations are going to be useful:

$$(\epsilon_{ij}^d)^2 + (\epsilon_{ij}^d)^{*2} = \frac{(\epsilon_A^d)_{ij}^2 + (\epsilon_V^d)_{ij}^2}{2}$$

$$= \left(\frac{2N}{vs_\beta} \right)^2 \left[(m_{d_i} + m_{d_j})^2 (C_d^A)_{ij}^2 + (m_{d_i} - m_{d_j})^2 (C_d^V)_{ij}^2 \right], \quad (2.28)$$

$$\begin{aligned} 2\epsilon_{ij}^d (\epsilon_{ij}^d)^* &= \frac{(\epsilon_A^d)_{ij}^2 - (\epsilon_V^d)_{ij}^2}{2} \\ &= \left(\frac{2N}{vs_\beta} \right)^2 \left[(m_{d_i} + m_{d_j})^2 (C_d^A)_{ij}^2 - (m_{d_i} - m_{d_j})^2 (C_d^V)_{ij}^2 \right]. \end{aligned} \quad (2.29)$$

Again, the analogous expressions for charged leptons are obtained by replacing $d \rightarrow e$, while for the up-quark sector by sending $d \rightarrow u$ and $s_\beta \rightarrow c_\beta$ in Eqs. (2.28)–(2.29).

2.4 Non-universal PQ-2HDM Yukawa textures

The relations derived in the previous section hold for a general non-universal PQ-2HDM. On the other hand, it is useful to provide for the following phenomenological analysis a couple of benchmark Yukawa textures that can nicely exemplify the IR/UV flavour correlation. Here, we will consider two explicit examples of 2+1-type models, i.e. with at least two generations featuring the same PQ charges, originally presented in Ref. [21] (see also [45]) in order to suppress the axion couplings to nucleons. Despite the reasons behind their original motivation, these two textures, labelled respectively as M1 and M4 in Ref. [21], are prototypes of models with quark flavour violation in axion couplings, respectively in the left-handed (LH) and in the right-handed (RH) down-quark sector. The lepton sector is more model-dependent and we report here for definiteness just one of the possible choices. Note that in these models it is also possible to achieve electrophobia via a tuning involving the rotation matrices of the charged leptons [21], thus realizing the so-called “astrohobic” axion scenario in which both coupling to nucleons and electrons are suppressed, and astrophysical axion bounds are in turn suppressed. The M1 and M4 textures are defined by the following Yukawa matrices:

- M1 model

$$Y_1^u = \begin{pmatrix} y_{11}^u & y_{12}^u & y_{13}^u \\ y_{21}^u & y_{22}^u & y_{23}^u \\ 0 & 0 & 0 \end{pmatrix}, \quad Y_2^u = \begin{pmatrix} 0 & 0 & 0 \\ 0 & 0 & 0 \\ y_{31}^u & y_{32}^u & y_{33}^u \end{pmatrix}, \quad (2.30)$$

$$Y_1^d = \begin{pmatrix} 0 & 0 & 0 \\ 0 & 0 & 0 \\ y_{31}^d & y_{32}^d & y_{33}^d \end{pmatrix}, \quad Y_2^d = \begin{pmatrix} y_{11}^d & y_{12}^d & y_{13}^d \\ y_{21}^d & y_{22}^d & y_{23}^d \\ 0 & 0 & 0 \end{pmatrix}, \quad (2.31)$$

$$Y_1^e = \begin{pmatrix} y_{11}^e & y_{12}^e & y_{13}^e \\ y_{21}^e & y_{22}^e & y_{23}^e \\ 0 & 0 & 0 \end{pmatrix}, \quad Y_2^e = \begin{pmatrix} 0 & 0 & 0 \\ 0 & 0 & 0 \\ y_{31}^e & y_{32}^e & y_{33}^e \end{pmatrix}. \quad (2.32)$$

Upon a baryon and lepton number transformation one can set $\mathcal{X}_{q_\alpha} = \mathcal{X}_{\ell_\alpha} = 0$ ($\alpha = 1, 2$), so that the PQ charge matrices satisfying the constraints in Eqs. (2.2)–(2.4) read

$$\begin{aligned} \mathcal{X}_q &= \text{diag}(0, 0, 1), \quad \mathcal{X}_u = \text{diag}(s_\beta^2, s_\beta^2, s_\beta^2), \quad \mathcal{X}_d = \text{diag}(c_\beta^2, c_\beta^2, c_\beta^2), \\ \mathcal{X}_\ell &= -\mathcal{X}_q, \quad \mathcal{X}_e = -\mathcal{X}_u. \end{aligned} \quad (2.33)$$

which shows that in the M1 model only the PQ charges in the quark and lepton LH sectors are non-universal.

- M4 model

$$Y_1^u = \begin{pmatrix} y_{11}^u & y_{12}^u & y_{13}^u \\ y_{21}^u & y_{22}^u & y_{23}^u \\ y_{31}^u & y_{32}^u & y_{33}^u \end{pmatrix}, \quad Y_2^u = 0, \quad (2.34)$$

$$Y_1^d = \begin{pmatrix} 0 & y_{12}^d & y_{13}^d \\ 0 & y_{22}^d & y_{23}^d \\ 0 & y_{32}^d & y_{33}^d \end{pmatrix}, \quad Y_2^d = \begin{pmatrix} y_{11}^d & 0 & 0 \\ y_{21}^d & 0 & 0 \\ y_{31}^d & 0 & 0 \end{pmatrix}, \quad (2.35)$$

$$Y_1^e = \begin{pmatrix} y_{11}^e & y_{12}^e & y_{13}^e \\ 0 & 0 & 0 \\ 0 & 0 & 0 \end{pmatrix}, \quad Y_2^e = \begin{pmatrix} 0 & 0 & 0 \\ y_{21}^e & y_{22}^e & y_{23}^e \\ y_{31}^e & y_{32}^e & y_{33}^e \end{pmatrix}. \quad (2.36)$$

Setting $\mathcal{X}_{q_1} = \mathcal{X}_{\ell_1} = 0$ via a baryon and lepton number transformation, the PQ charges in the M4 model are fixed to be

$$\begin{aligned} \mathcal{X}_q &= \text{diag}(0, 0, 0), & \mathcal{X}_u &= \text{diag}(s_\beta^2, s_\beta^2, s_\beta^2), & \mathcal{X}_d &= \text{diag}(c_\beta^2, -s_\beta^2, -s_\beta^2), \\ \mathcal{X}_\ell &= -\text{diag}(0, 1, 1), & \mathcal{X}_e &= -\mathcal{X}_u, \end{aligned} \quad (2.37)$$

which imply non-universality in the RH down sector and in the LH lepton sector.

With the specific choice of the trilinear $H_2^\dagger H_1 \phi$ term in the scalar potential, one has $2N = 1$ both in the M1 and M4 models. Flavour violating axion couplings to fermions (as defined in Eq. (2.8)) arise exclusively in the LH sector for the M1 model, i.e.

$$(C_u^{V,A})_{i \neq j} = \pm (V_{u_L}^\dagger \mathcal{X}_q V_{u_L})_{i \neq j}, \quad (2.38)$$

$$(C_d^{V,A})_{i \neq j} = \pm (V_{d_L}^\dagger \mathcal{X}_q V_{d_L})_{i \neq j}, \quad (2.39)$$

$$(C_e^{V,A})_{i \neq j} = \pm (V_{e_L}^\dagger \mathcal{X}_\ell V_{e_L})_{i \neq j}, \quad (2.40)$$

while for the M4 model flavour violation arises in the RH down-quark sector and LH charged-lepton sector respectively:

$$(C_u^{V,A})_{i \neq j} = 0, \quad (2.41)$$

$$(C_d^{V,A})_{i \neq j} = (V_{d_R}^\dagger \mathcal{X}_d V_{d_R})_{i \neq j}, \quad (2.42)$$

$$(C_e^{V,A})_{i \neq j} = \pm (V_{e_L}^\dagger \mathcal{X}_\ell V_{e_L})_{i \neq j}. \quad (2.43)$$

Moreover, the combination of flavour violating couplings appearing in $\Delta F = 2$ observables, defined in Eqs. (2.28)–(2.29), take the simpler form (both in the M1 and M4 models)

$$(\epsilon_{ij}^d)^2 + (\epsilon_{ij}^d)^*{}^2 = 2 \left(\frac{1}{vs_\beta} \right)^2 (m_{d_i}^2 + m_{d_j}^2) (C_d^{V,A})_{ij}^2, \quad (2.44)$$

$$2 \epsilon_{ij}^d (\epsilon_{ij}^d)^* = 4 \left(\frac{1}{vs_\beta} \right)^2 m_{d_i} m_{d_j} (C_d^{V,A})_{ij}^2, \quad (2.45)$$

with the analogous expressions for the up-quark sector obtained by replacing $d \rightarrow u$ and $s_\beta \rightarrow c_\beta$.

3 Flavour phenomenology

With the aid of the relations obtained in the previous section we can now investigate the interplay between axion flavour phenomenology and the signatures arising from the heavy Higgs radial modes of the PQ-2HDM. We start by discussing LHC constraints on low-scale, i.e. $\mathcal{O}(1 \text{ TeV})$, 2HDM and then consider all relevant flavour bounds on the non-universal PQ-2HDM, both in the quark and lepton sectors. This phenomenological analysis actually applies to a general 2HDM with tree-level flavour changing couplings, regardless of the presence of the PQ symmetry. All the details regarding the 2HDM potential and its mass spectrum are deferred to Appendix A, while the analysis of meson mixing and a collection of formulae for LFV processes can be found in Appendix C and E. Finally, based on the IR/UV flavour connection (cf. Eqs. (2.22)–(2.24)), we discuss the consequences of an axion discovery in flavour violating decays on the PQ-2HDM parameter space.

3.1 LHC bounds on the 2HDM

The 2HDM scalar sector can be tested at the LHC in two different ways: either indirectly via the modification of Higgs couplings or by directly hunting for new scalar resonances. The first type of searches are only sensitive to the mixing angles in the scalar sector, while direct searches are also sensitive to the typical mass scale of the enlarged scalar sector.

LHC Higgs data implies that the observed properties of the $h(125)$ resonance are very close to those predicted by the SM. In particular, observables such as Higgs couplings to fermions and SM gauge bosons yield already a robust upper bound on the rotation matrix that diagonalize the neutral scalar sector, $c_{\alpha-\beta} \lesssim 0.3(0.1)$ [46] for a type-I(II) 2HDM [47].⁴

In order to automatically satisfy LHC constraints on Higgs couplings, the so-called SM *alignment* limit [48] has been introduced, in which one of the two Higgs doublets is nearly aligned with the electroweak VEV, thus reproducing the properties of a SM-like Higgs. There are basically two ways of achieving alignment. The first one is *alignment with decoupling*, in which the condition $c_{\alpha-\beta} \rightarrow 0$ is obtained by decoupling all the heavy radial modes, $m_H \simeq m_A \simeq m_{H^\pm} \gg m_h$ (cf. Eq. (A.31)). In this case we identify h and H respectively as the SM-like and non-SM-like Higgs scalars. *Alignment without decoupling* is obtained, instead, by taking the scalar potential parameter $\Lambda_6 \rightarrow 0$ which allows for a second light Higgs in the spectrum with a mass either larger [49] (if $c_{\alpha-\beta} \rightarrow 0$) or smaller [50] (if $s_{\alpha-\beta} \rightarrow 0$) than the observed scalar resonance at 125 GeV. The field H then labels the non-SM-Higgs (SM-Higgs) in the first (latter) eventuality. Notice that in the alignment without decoupling scenario the mass spectrum of the scalar particles is not necessarily degenerate and it is determined, in particular, by the parameter Λ_5 of the scalar potential. Hereafter, we will only consider the case $m_H \gtrsim m_h$ (i.e. $c_{\alpha-\beta} \simeq 0$) and therefore h will always denote the SM-like Higgs.

LHC has also greatly contributed to direct searches for an extended scalar sector, looking for both neutral [51–69] and charged scalar particles [70–73]. Different mechanisms can be responsible for the production of new scalar resonances: *i*) Vector Boson Fusion (VBF) is proportional to $c_{\alpha-\beta}$ and hence substantially suppressed in the alignment limit, *ii*) gluon-gluon Fusion (ggF) depends, instead, parametrically on t_β and therefore bottom quarks can contribute sizeably to ggF. Direct and indirect searches, as well as different production mechanisms are hence used to give bounds on the 2HDM in the (m_X, t_β) plane (where $X = H, A, H^\pm$), for a given value of $c_{\alpha-\beta}$. For instance, searches for scalar particle decays into gauge bosons test the lower parts of the (m_X, t_β) plane for type-I and II models [52–55, 59, 64], while type-II enhanced di- τ decay set a strong upper bound on t_β [51, 60]. For recent analyses on the parameter space of the 2HDM, see e.g. [74–76]. In particular, a recent global fit to type-II 2HDM [76] shows that $m_H \gtrsim 500$ GeV independently of t_β , while the bound stretches up to $m_H \simeq 1$ TeV for $t_\beta \gtrsim 1$.

One can partially use type-I and II 2HDM collider searches to provide approximate bounds for the non-universal PQ-2HDM models by applying the present limits on the 33 entries of the Yukawa matrices ($y_{t,b,\tau}$) of the benchmark M1 and M4 models introduced in Section 2. In this approximation the type-I and II models searches can be related to the M1 and M4 Yukawa structures, as summarized in Table 1 for the 3rd generation fermion couplings to the H scalar field. However, although M1 and M4 models behave only partially as type-I and II 2HDM, in the following, as a conservative approach, we will regardless employ bounds from the type-II model, which turn out to be more stringent.

⁴Recall that (universal) 2HDM's with natural flavour conservation are conventionally classified as *i*) type-I model if only one of the two scalar doublets couples (universally) to all fermions or *ii*) type-II model if up- and down-quarks sectors couple to different doublets. In particular, the (universal) DFSZ axion model is compatible only with the type-II structure.

Model	y_t	y_b	y_τ
Type-I	$\frac{s_\alpha}{s_\beta}$	$\frac{s_\alpha}{s_\beta}$	$\frac{s_\alpha}{s_\beta}$
Type-II	$\frac{s_\alpha}{s_\beta}$	$\frac{c_\alpha}{c_\beta}$	$\frac{c_\alpha}{c_\beta}$
M1	$\frac{s_\alpha}{s_\beta}$	$\frac{c_\alpha}{c_\beta}$	$\frac{s_\alpha}{s_\beta}$
M4	$\frac{c_\alpha}{c_\beta}$	$\frac{s_\alpha}{s_\beta}$	$\frac{c_\alpha}{c_\beta}$

Table 1: Scaling of the H couplings to 3rd generation SM fermions, in the type-I and II 2HDM compared to the M1 and M4 models. Type-I (II) couplings are emphasized in blue (red), while grey shaded couplings have no counterpart in universal 2HDMs. Couplings which are the same in both models are colored in purple.

3.2 Flavour constraints on the non-universal 2HDM

The strongest constraints on the quark flavour violating couplings of the heavy radial modes of the PQ-2HDM arise from neutral mesons mixing. The parameter space of a flavourful 2HDM has been previously studied also in connection with LHC data (see for example [77]). Previous analyses often relied on Yukawa textures specifically introduced in order to suppress tree-level flavour changing neutral currents (FCNCs), as e.g. in the case of the Cheng-Sher ansatz [78]. In this Section, conversely, we do not assume any particular form for the Yukawa matrices, and perform, instead, an analysis of meson mixing constraints on the parameter space of a general 2HDM with tree-level flavour-changing couplings. Our numerical analysis, including QCD running effects, follows the one in Ref. [77] (see also [79–81]). Additionally, we take into account (whenever available) the theoretical error on the SM predictions for the meson mixing parameters. In the case of B systems theoretical uncertainties are at the level of $\sim 5\%$ [82], while Kaon physics has not yet reached this level of precision and lattice calculations provide K -form factors with an $\mathcal{O}(30\%)$ error, see for example Refs. [83, 84].

The details of the analysis are reported in Appendix C. Here, we summarize the main results in the alignment scenario, which is necessary in order to satisfy LHC constraints on $c_{\alpha-\beta}$. The bounds from meson mixing can be recast in this limit as

$$\left(\frac{[4.1, 3.6] \text{ TeV}}{s_{2\beta} m_H} \right)^2 \frac{m_H^2 + m_A^2}{2m_A^2} \left| \frac{\epsilon_{12}^d \epsilon_{21}^{d*}}{y_s^2 \lambda^2} + 0.12 \frac{m_H^2 - m_A^2}{m_H^2 + m_A^2} \frac{(\epsilon_{12}^d)^2 + (\epsilon_{21}^{d*})^2}{y_s^2 \lambda^2} \right| < 1, \quad (3.1)$$

$$\left(\frac{[1.4, 1.7] \text{ TeV}}{s_{2\beta} m_H} \right)^2 \frac{m_H^2 + m_A^2}{2m_A^2} \left| \frac{\epsilon_{13}^d \epsilon_{31}^{d*}}{y_b^2 \lambda^6} + 0.17 \frac{m_H^2 - m_A^2}{m_H^2 + m_A^2} \frac{(\epsilon_{13}^d)^2 + (\epsilon_{31}^{d*})^2}{y_b^2 \lambda^6} \right| < 1, \quad (3.2)$$

$$\left(\frac{[1.5, 1.6] \text{ TeV}}{s_{2\beta} m_H} \right)^2 \frac{m_H^2 + m_A^2}{2m_A^2} \left| \frac{\epsilon_{23}^d \epsilon_{32}^{d*}}{y_b^2 \lambda^4} + 0.17 \frac{m_H^2 - m_A^2}{m_H^2 + m_A^2} \frac{(\epsilon_{23}^d)^2 + (\epsilon_{32}^{d*})^2}{y_b^2 \lambda^4} \right| < 1, \quad (3.3)$$

$$\left(\frac{23 \text{ TeV}}{m_H} \right)^2 \frac{m_H^2 + m_A^2}{2m_A^2} \left| \frac{\epsilon_{12}^u \epsilon_{21}^{u*}}{y_c^2 \lambda^2} + 0.15 \frac{m_H^2 - m_A^2}{m_H^2 + m_A^2} \frac{(\epsilon_{12}^u)^2 + (\epsilon_{21}^{u*})^2}{y_c^2 \lambda^2} \right| < 1, \quad (3.4)$$

where we have equated the contribution of the Wilson coefficients of the relevant 4-fermion operators to the mass scale written in the bracket and rescaled the UV sources of flavour violation ($\epsilon^{u,d}$) with suitable powers of Yukawas, $y_{d_i(u_i)} = \frac{\sqrt{2}m_i}{vs_\beta(c_\beta)}$, and Cabibbo angle, λ . This rescaling corresponds to a CKM-like structure for the LH rotation matrices, $V_{u_L} \sim V_{d_L} \sim V_{\text{CKM}}$, and $V_{u_R} \sim V_{d_R} \sim \mathbb{1}$ for the RH ones. For example, in Eq. (3.4) one has $\epsilon_{12}^u = (V_{u_L}^\dagger Y_1^u V_{u_R})_{12} \sim (V_{u_L})_{12}^* (Y_1^u)_{22} (V_{u_R})_{22} \sim \lambda \frac{\sqrt{2}m_c}{v c_\beta}$. To obtain the numerical values reported in Eqs. (3.1)–(3.4)

we have used the PDG values for $m_i(\mu)$, with $\mu = \{2, 2.8, 4.6\}$ GeV respectively for K , D and B meson oscillations and $\lambda = 0.2$. For down-type flavour transitions, where reliable SM theoretical predictions are available, the number quoted in the left (right) of the square bracket corresponds to a negative (positive) contribution from new physics. For $D^0 - \bar{D}^0$ oscillation we have required, instead, that the new physics contribution would not overshoot the available experimental bound.

Note that one of the mass terms (e.g. m_A) can be traded, via Eq. (A.32), for the scalar potential parameter Λ_5 , subject to the perturbativity constraint $\Lambda_5 \lesssim 4\pi$. The alignment scenario with decoupling is readily recovered by taking the $m_H^2 \rightarrow m_A^2$ limit in Eqs. (3.1)–(3.4).

Employing a CKM-like structure for the fermion rotation matrices, we have studied the implication of the meson mixing bounds on the benchmark models M1 and M4 (see Appendix D for details). In summary, the CKM suppression is sufficient in order to make these models accessible at the LHC. For M1 the bound from meson mixing is $m_H \gtrsim 200$ GeV, while for M4 is $m_H \gtrsim 1$ TeV. This shows that, despite having FCNCs at tree level, certain PQ charge arrangements and flavour ansatz can relax the bounds on the mass scale of the (non-universal) 2HDM, similarly to the case of BGL models [85] (see also [86]). In Appendix D we have also considered the meson mixing bounds induced by the SM-like Higgs in the $(c_{\alpha-\beta}, t_\beta)$ plane, in the case in which the heavy Higgs (H) is not completely decoupled. These bounds are found to constrain similar regions of parameter space, as those arising from the SM-like Higgs LFV decays, considered in Ref. [37].

Regarding instead the leptonic sector of the (non-universal) 2HDM with tree-level FCNCs, we can mostly rely on previous analyses, such as those in Refs. [87, 88]. Indeed, the bounds from $l_i \rightarrow l_j \gamma$ [89, 90] have been only marginally improved [91, 92]; while leptonic decays of the type $l_i \rightarrow 3l_j$ or $l_i \rightarrow l_j l_k l_k$ are still based on the SINDRUM [93] and Belle [94] experiments, also taken into account in [88]. On the other hand, the limits on Higgs LFV decays have been considerably improved in the recent years by the LHC [95, 96]. In particular, very strong limits on the parameter space of the (non-universal) 2HDM arise from the $h \rightarrow \tau \mu$ and $h \rightarrow \tau e$ processes, while for the case of μ - e transitions $\mu \rightarrow e \gamma$ still provides the most relevant constraint. The Higgs LFV branching ratios, in the notation of Eq. (2.12), read

$$\text{BR}(h \rightarrow l_i l_j) = \frac{m_h}{16\pi\Gamma_h} (|C_{ij}^{h_e}|^2 + |C_{ji}^{h_e}|^2), \quad (3.5)$$

where Γ_h could receive corrections from new physics (cf. Eq. (E.9)). By means of Eq. (2.13) we can rewrite the 2σ bound from $h \rightarrow \tau \mu/e$ directly on the ϵ^e coefficients as

$$\frac{4.1 \text{ MeV}}{\Gamma_h} \frac{|\epsilon_{i3}^e|^2 + |\epsilon_{3i}^e|^2}{y_\tau^2} \left(\frac{c_{\alpha-\beta}}{s_\beta c_\beta} \right)^2 \lesssim 0.066, \quad (3.6)$$

where $i = 1, 2$ (since at 2σ both the μ and e channels yield a similar bound) and $y_\tau = \sqrt{2}m_\tau/vs_\beta$. The Higgs branching ratio has been normalized to the SM model one, $\Gamma_h^{\text{SM}} \simeq 4.1 \text{ MeV}$.

3.3 IR/UV quark flavour connection

As seen in Section 2.3 there is a direct relation between the IR sources of flavour violation ($C_f^{V,A}$) and the UV ones ($\epsilon_{V,A}^f$). This is particularly useful in the case of a positive detection of a new physics effect, since once the strength of the flavour violation is known in one of the two sectors, it can be directly translated into the other one. The second important point is the generality of these correlations. While the flavour violating axion signals depend on the specific model via the PQ charges and the fermion mixing matrices $V_{fL/R}$, the correlations derived in Section 2.3 are model-independent, in the sense that they directly relate the flavour coefficients entering the physical observables.

In the following, we highlight the IR/UV connection in a class of non-universal PQ models with a 2+1 structure of the PQ charges, like the M1 and M4 models introduced in Section 2.4, exemplifications of scenarios in which flavour violation in the axion couplings arises either in the LH or RH sector. The generalization to the most general setup with both LH and RH flavour violation is then straightforward. Through Eqs. (2.28)–(2.29) we can directly translate the information on the PQ symmetry breaking scale f_a , appearing explicitly in the IR axion couplings to fermions into limits on the heavy 2HDM scale m_H (and t_β) by relating flavour violating axion observables with meson mixing ones:

$$\left(\frac{f_a}{10^{11} \text{ GeV}}\right)^2 \left(\frac{1 \text{ TeV}}{s_{2\beta} m_H}\right)^2 \left(\frac{\text{BR}(K \rightarrow \pi a)}{7.3 \cdot 10^{-11}}\right) = \frac{2 |M_{12}^{\text{NP}}|}{3.5 \cdot 10^{-15} \text{ GeV}}, \quad (3.7)$$

$$\left(\frac{f_a}{2.8 \cdot 10^7 \text{ GeV}}\right)^2 \left(\frac{1 \text{ TeV}}{s_{2\beta} m_H}\right)^2 \left(\frac{\text{BR}(B \rightarrow \pi a)}{2.3 \cdot 10^{-5}}\right) = \frac{2 |M_{12}^{\text{NP}}|}{3.3 \cdot 10^{-13} \text{ GeV}}, \quad (3.8)$$

$$\left(\frac{f_a}{8.8 \cdot 10^7 \text{ GeV}}\right)^2 \left(\frac{1 \text{ TeV}}{s_{2\beta} m_H}\right)^2 \left(\frac{\text{BR}(B \rightarrow K a)}{7.1 \cdot 10^{-6}}\right) = \frac{2 |M_{12}^{\text{NP}}|}{1.2 \cdot 10^{-11} \text{ GeV}}, \quad (3.9)$$

$$\left(\frac{f_a}{1.2 \cdot 10^7 \text{ GeV}}\right)^2 \left(\frac{1 \text{ TeV}}{s_{2\beta} m_H}\right)^2 \left(\frac{\text{BR}(D \rightarrow \pi a)}{8 \cdot 10^{-6}}\right) = \frac{2 |M_{12}^{\text{NP}}|}{6.7 \cdot 10^{-15} \text{ GeV}}. \quad (3.10)$$

These expressions have been written, for simplicity, in the alignment limit (i.e. $c_{\alpha-\beta} \simeq 0$) assuming $m_H^2 \simeq m_A^2$. Flavour violating axion observables and meson mixing parameters have been normalized to current experimental limits. In particular, the 90% CL limits on the branching ratios involving the axion field are taken from Ref. [28].

The connections established in Eqs. (3.7)–(3.10) fully prove their relevance once an evidence of deviation from the SM will emerge. Assuming, for example, an axion discovery in a given flavour violating meson decay, it will be then straightforward to relate it to a possible deviation from SM predictions in meson mixing observables, induced by the heavy radial modes of the PQ-2HDM.⁵ Fixing the branching ratio of the flavour violating axion observable in a region between the current experimental bound and the future expected sensitivity (the latter is also taken from Ref. [28]), we can translate the current bound imposed by meson mixing into a relation of the type $f_a < \#_{f_a} s_{2\beta} m_H$, with $\#_{f_a}$ a number which can be read directly from Eqs. (3.7)–(3.10) (or equivalently $m_a > \#_{m_a} s_{2\beta} m_H$, using the QCD axion mass relation, $m_a \simeq 5.7 \times (10^6 \text{ GeV}/f_a) \text{ eV}$). This region corresponds the white upper-right half-plane in the plots of Figs. 1–2, where we also superimpose LHC constraints and astrophysical bounds on the axion decay constant. In the latter case we assume two scenarios corresponding to a suppressed axion coupling to nucleons and electrons (astrophobic scenario [21]) and $C_e = 1$ (corresponding to a sizeable value of the axion coupling to electrons).

If the axion is discovered in the near future (i.e. in the region between current bounds and future sensitivities) in B - or D -meson transitions, it is evident from Figs. 1–2 that the interplay of meson mixing and astrophysical bounds disfavour the possibility of probing the radial modes of the PQ-2HDM at the LHC (unless the axion is to some extent astrophobic). On the other hand, a discovery of the axion in $K \rightarrow \pi a$ leaves open plenty of parameter space for a light PQ-2HDM in the LHC range, since astrophysical constraints are not relevant for large f_a .

A similar discussion applies if a SM deviation will be detected in meson mixing. In such a case Figs. 1–2 would be filled in the upper-right plane, and one could draw well-definite conclusions regarding the possibility to observe an axion within the reach of current or future meson decay experiments. This scenario is however more difficult to be realized in practice, since it relies on a precise SM computation for the meson mixing parameters.

⁵Note that meson mixing receives also an IR contribution from the tree-level exchange of the axion field. However, this contribution is subleading compared to the UV-induced one, as long as $f_a \gg m_H$.

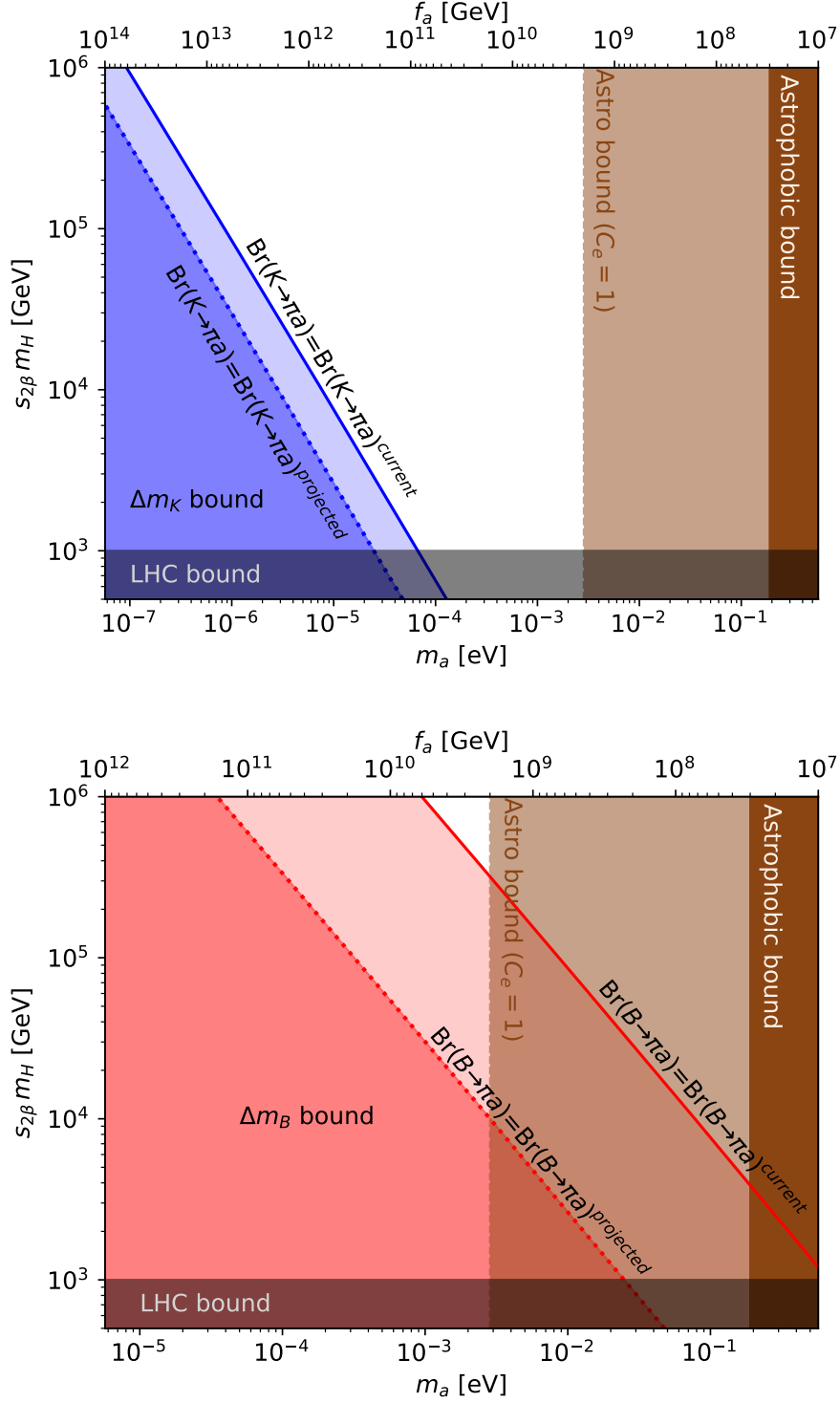


Figure 1: IR/UV quark flavour connection in the $(m_a, s_{2\beta} m_H)$ plane, assuming an axion discovery in a given flavour transition, with solid (dotted) lines corresponding to current bounds (future sensitivities) on meson decays. The upper-right region is allowed by current bounds on K^0 (upper plot) and B_d^0 (lower plot) meson mixing. LHC bounds (set approximately at 1 TeV) are displayed in grey, while the brown regions correspond to astrophysical bounds on the axion decay constant, between $f_a \sim 3 \times 10^7$ GeV (astrophobic scenario) and $f_a \sim 2 \times 10^9$ GeV, an axion with a sizeable coupling to electrons ($C_e = 1$).

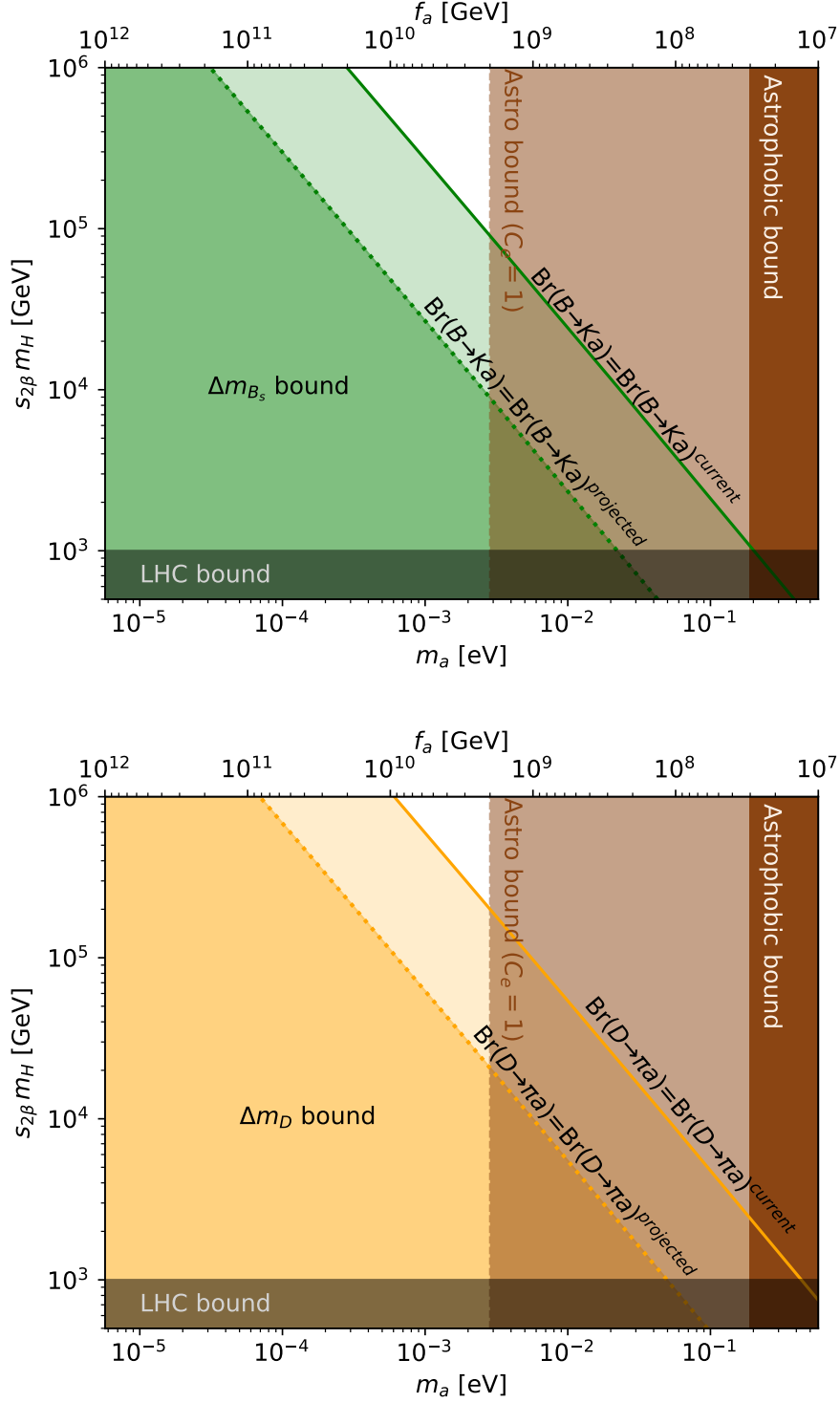


Figure 2: IR/UV quark flavour connection in the $(m_a, s_{2\beta} m_H)$ plane, assuming an axion discovery in a given flavour transition, with solid (dotted) lines corresponding to current bounds (future sensitivities) on meson decays. The upper-right region is allowed by current bounds on B_s^0 (upper plot) and D^0 (lower plot) meson mixing. LHC bounds (set approximately at 1 TeV) are displayed in grey, while the brown regions correspond to astrophysical bounds on the axion decay constant, between $f_a \sim 3 \times 10^7$ GeV (astrophobic scenario) and $f_a \sim 2 \times 10^9$ GeV, an axion with a sizeable coupling to electrons ($C_e = 1$).

i, j	$\text{BR}(h \rightarrow l_i l_j)$	Current $\text{BR}(l_i \rightarrow a l_j)$	Expected $\text{BR}(l_i \rightarrow a l_j)$
τ, e	$0.09 \pm 0.06 \%$ [96]	9.4×10^{-4} [98]	8.3×10^{-6} [29]
τ, μ	$0.11^{+0.05}_{-0.04} \%$ [96]	5.9×10^{-4} [98]	2.0×10^{-5} [29]

Table 2: Input values used in the LFV analysis in Fig. 3. Lepton decays correspond to 95% CL bounds, while the Higgs branching ratios are measurements at 1σ .

3.4 IR/UV lepton flavour connection

In the charged-lepton sector it is possible to exploit Eq. (2.24) in order to connect LFV axion processes like $l_i \rightarrow l_j a$ with other LFV observables such as $l_i \rightarrow 3l_j$, $l_i \rightarrow l_j l_k l_k$ and $l_i \rightarrow l_j \gamma$. However, as shown in Appendix E, the relation between this two classes of LFV observables is not straightforward as in the quark case considered in Section 3.3, because of the appearance of several couplings which break the 1-to-1 flavour correspondence. Hence, a global analysis would be necessary in this case.

Another possibility is to consider LFV Higgs decays $h \rightarrow l_i l_j$, which actually turns out to be in direct connection with LFV axion processes, thus providing a useful simplification. Moreover, there is a recent hint from ATLAS [96] about a possible deviation from the SM in the Higgs branching ratios $\text{BR}(h \rightarrow \tau e) = 0.09 \pm 0.06 \%$ and $\text{BR}(h \rightarrow \tau \mu) = 0.11^{+0.05}_{-0.04} \%$. These provide indeed a useful benchmark in order to highlight the IR/UV lepton flavour connection. Note, also, that deviations at the 0.1% level in $\text{BR}(h \rightarrow \tau e/\mu)$ within a non-universal 2HDM are still allowed by other LFV observables (see e.g. [97]). Employing Eq. (3.5) and the IR/UV connection formulae in Section 2.3, we obtain the following expression for the LFV Higgs decays in terms of axion couplings

$$\text{BR}(h \rightarrow l_i l_j) \simeq \frac{m_h}{16\pi\Gamma_h} \left(\frac{c_{\alpha-\beta}}{s_\beta c_\beta} \right)^2 \frac{m_{l_i}^2}{v^2} |(C_e^{L,R})_{ij}|^2, \quad (3.11)$$

which applies to models with 2+1 PQ charges (the extension to general non-universal DFSZ models, with both LH and RH axion flavour violation, is provided in Eq. (E.8)). Given a LFV process involving the axion field [29]

$$\text{BR}(l_i \rightarrow l_j a) \simeq \frac{m_{l_i}^3}{16\pi\Gamma_{l_i}} \frac{|(C_e^{L,R})_{ij}|^2}{2f_a^2}, \quad (3.12)$$

we can provide a direct relation for the two branching ratios, that reads

$$\text{BR}(h \rightarrow l_i l_j) \simeq \text{BR}(l_i \rightarrow a l_j) \frac{2m_h}{m_{l_i}} \frac{\Gamma_{l_i}}{\Gamma_h} \frac{f_a^2}{v^2} \left(\frac{c_{\alpha-\beta}}{c_\beta s_\beta} \right)^2. \quad (3.13)$$

Employing the data in Table 2, we display in Fig. 3 the correlation provided by Eq. (3.13) in the $(m_a, c_{\alpha-\beta}/s_{2\beta})$ plane. Assuming as a benchmark the hint from ATLAS on $h \rightarrow \tau\mu/e$ decays, we impose the bounds and future sensitivities from the axion processes $\tau \rightarrow ea$ (top panel) and $\tau \rightarrow \mu a$ (bottom panel), as well as reference astrophysical limits on the axion mass and LHC constraints on $c_{\alpha-\beta}$ for typical model parameters. The combination of all bounds corners a region of the axion mass parameter space that will be targeted by future axion searches (such as those with helioscopes) and that is characterized by a remarkable complementarity between different types of observables, ranging from flavour physics and LHC direct searches to axion astrophysics.

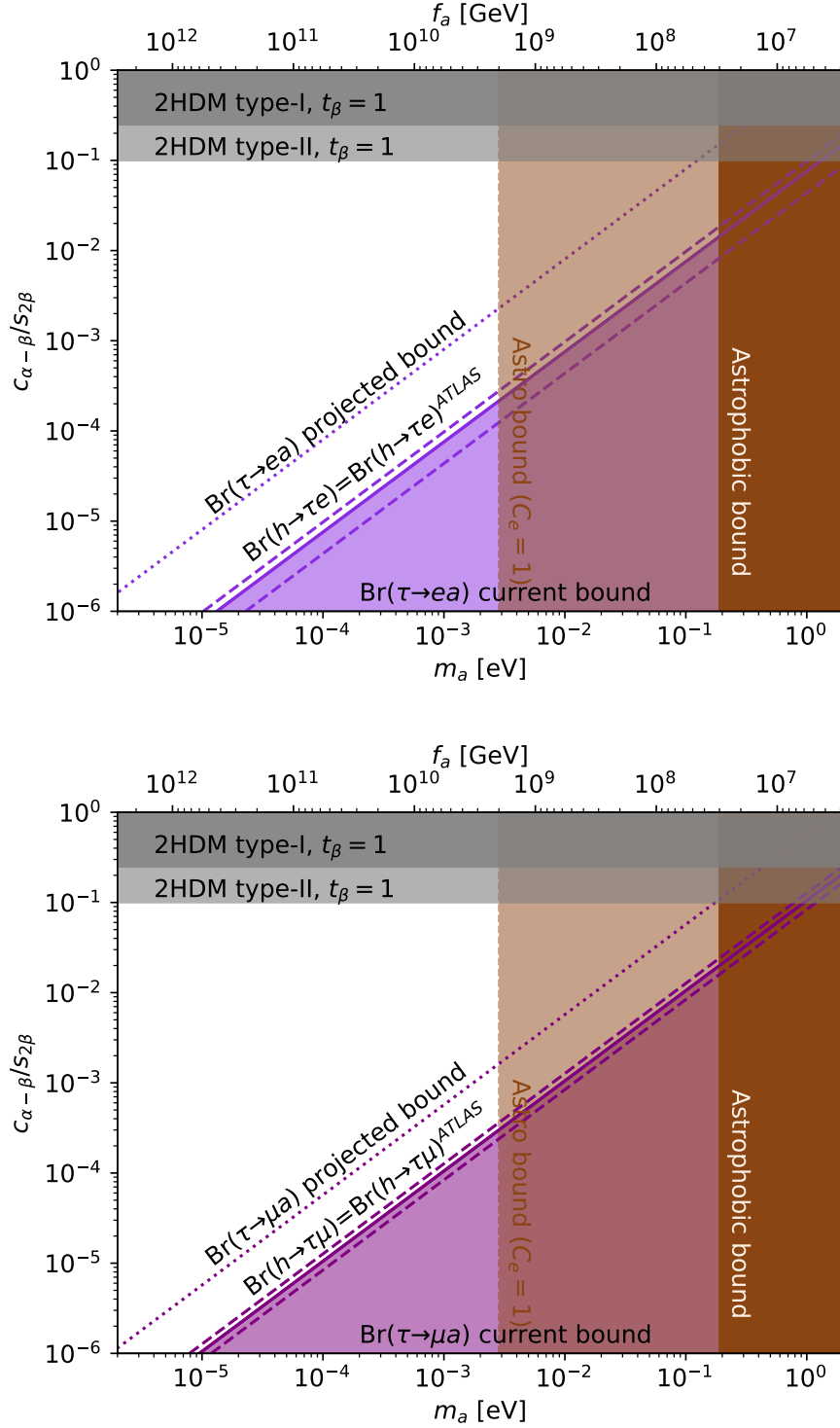


Figure 3: IR/UV lepton flavour connection in the $(m_a, c_{\alpha-\beta}/s_{2\beta})$ plane, assuming the hint on LFV Higgs decays $h \rightarrow \tau\mu/e$ and imposing the bound (colored purple region being excluded) from $\tau \rightarrow ea$ (top panel) and $\tau \rightarrow \mu a$ (bottom panel). Solid (dotted) lines correspond to current bounds (future sensitivities) from τ decays, while dashed lines refer to the 1σ region for the $h \rightarrow \tau\mu/a$ hint. For input data see Table 2. LHC bounds on $c_{\alpha-\beta}$ (for $t_\beta = 1$) are displayed in grey as a reference in the case of the type-I and -II 2HDM, while the brown regions correspond to astrophysical bounds on the axion decay constant, between $f_a \sim 3 \times 10^7$ GeV (astrophobic scenario) and $f_a \sim 2 \times 10^9$ GeV, for an axion with a sizeable coupling to electrons ($C_e = 1$).

4 Conclusions

In this paper we have studied the flavour phenomenology of non-universal DFSZ axion models, focusing on the interplay between IR and UV sources of flavour violation. These consist respectively in the flavour violating axion couplings to fermions, whose chiral counterparts are denoted as $C_f^{L,R}$ (see Eq. (2.8)) and the flavour violating couplings of the heavy radial modes of the PQ-2HDM, which are expressed in terms of the ϵ^f parameters (defined in Eq. (2.17)). The key relations, providing a direct link between the ϵ^f and $C_f^{L,R}$ coefficients, are given by Eqs. (2.22)–(2.24). These remarkably simple equations, that lock the flavour violating pattern of the axion field to that of the heavy radial modes, hold in general for any (non-universal) DFSZ models, with a renormalizable 2HDM embedded. In fact, in order to derive Eqs. (2.22)–(2.24) we have exploited the $U(1)_{PQ}$ invariance of the PQ-2HDM Yukawa sector made explicit in Eqs. (2.2)–(2.4).

With the help of Eqs. (2.22)–(2.24) we have hence investigated the flavour phenomenology both in the quark and charged-lepton sectors, also in connection with LHC limits on the PQ-2HDM and astrophysical constraints on axion couplings. In the quark sector we focused on meson mixing observables, which yield the strongest constraints on the flavour violating couplings of the non-universal PQ-2HDM radial modes. We have also derived a set of useful formulae (see Eqs. (3.1)–(3.4)), from which present bounds on meson mixing mass differences can be translated to tree-level flavour violating couplings of a general 2HDM in the alignment limit, regardless of the presence of the PQ symmetry.

In order to further exemplify the IR/UV flavour connection we have considered two explicit examples of 2+1 models, labelled M1 and M4, which are prototypes of models with quark flavour violation in axion couplings, respectively in the LH and in the RH down-quark sector. Assuming an axion discovery in flavour violating meson decays, and imposing in turn the bounds from meson mixing experiments we have obtained the results shown in Figs. 1–2. The main message that can be learnt with such exercise is that if an axion is discovered in the near future in B - or D -meson transitions, then the interplay of meson mixing and astrophysical bounds disfavors the possibility of probing the radial modes of the PQ-2HDM at the LHC. On the other hand, an axion discovery in $K \rightarrow \pi a$ leaves open plenty of parameter space for a light PQ-2HDM in the LHC range.

A similar IR/UV connection can be envisaged as well for the charged-lepton sector. However, LFV observables, such as for example $l_i \rightarrow l_j \gamma$, turn out to depend on several axion couplings, making a direct connection with LFV axion processes not straightforward. To this end, we have considered instead SM-like Higgs decays $h \rightarrow l_i l_j$, which actually provide a 1-to-1 flavour correspondence with LFV axion processes such as $l_i \rightarrow l_j a$. Given the fact that ATLAS [96] currently hints to a mild deviation from the SM in the Higgs decays $h \rightarrow \tau e / \mu$, we have taken this as a benchmark scenario and imposed the bounds from axion LFV processes, exploiting again the relation between IR and UV sources of flavour violation. The results of this analysis are displayed in Fig. 3, which shows again a strong complementarity between flavour observables, LHC direct searches and axion astrophysics.

Acknowledgements

We thank Mario Fernández Navarro, Belén Gavela, Luca Merlo and Robert Ziegler for useful discussions and comments. This work received funding from the European Union’s Horizon 2020 research and innovation programme under the Marie Skłodowska-Curie grant agreement N° 860881-HIDDeN, grant agreement N° 101086085-ASYMMETRY and by the INFN Iniziative Specifica APINE. The work of LDL is also supported by the project “CPV-Axion” under the Supporting TAlent in ReSearch@University of Padova (STARS@UNIPD).

A PQ-2HDM scalar potential

In this Appendix we provide some details on the scalar potential, with a special focus on the PQ-2HDM spectrum in the PQ broken phase (see also [99, 100]). The DFSZ scalar potential, in the presence of the cubic invariant $H_2^\dagger H_1 \phi$, can be written as

$$\begin{aligned} V(H_1, H_2, \phi) = & \mu_1^2 |H_1|^2 + \mu_2^2 |H_2|^2 + \frac{\lambda_1}{2} |H_1|^4 + \frac{\lambda_2}{2} |H_2|^4 + \lambda_3 |H_1|^2 |H_2|^2 \\ & + \lambda_4 (H_1^\dagger H_2)(H_2^\dagger H_1) + \frac{\lambda_1^\phi}{2} |\phi|^2 |H_1|^2 + \frac{\lambda_2^\phi}{2} |\phi|^2 |H_2|^2 + \lambda_3^\phi \left(|\phi|^2 - \frac{v_\phi^2}{2} \right)^2 \\ & - \left(\mu_\phi H_2^\dagger H_1 \phi + \text{h.c.} \right), \end{aligned} \quad (\text{A.1})$$

where the Higgs doublets are decomposed as

$$H_1 = \begin{pmatrix} \frac{1}{\sqrt{2}}(v_1 + h_1^0 + i\eta_1) \\ h_1^- \end{pmatrix}, \quad H_2 = \begin{pmatrix} \frac{1}{\sqrt{2}}(v_2 + h_2^0 + i\eta_2) \\ h_2^- \end{pmatrix}. \quad (\text{A.2})$$

In the PQ-broken phase, with $\langle \phi \rangle = v_\phi / \sqrt{2}$, we can integrate out the radial mode of the ϕ field and obtain the leading-order PQ-2HDM potential

$$\begin{aligned} V(H_1, H_2) = & m_{11}^2 |H_1|^2 + m_{22}^2 |H_2|^2 - \left(m_{12} H_1^\dagger H_2 + \text{h.c.} \right) \\ & + \frac{\lambda_1}{2} |H_1|^4 + \frac{\lambda_2}{2} |H_2|^4 + \lambda_3 |H_1|^2 |H_2|^2 + \lambda_4 (H_1^\dagger H_2)(H_2^\dagger H_1), \end{aligned} \quad (\text{A.3})$$

where

$$m_{11}^2 = \mu_1^2 + \frac{\lambda_1^\phi}{4} v_\phi^2, \quad m_{22}^2 = \mu_2^2 + \frac{\lambda_2^\phi}{4} v_\phi^2, \quad m_{12}^2 = \mu_\phi^* \frac{v_\phi}{\sqrt{2}}. \quad (\text{A.4})$$

To implement the $v_\phi \gg v$ hierarchy, we impose the “ultra-weak” scaling $\lambda_{1,2}^\phi \sim v^2/v_\phi^2$ and $\mu_\phi \sim v^2/v_\phi$, which also guarantees that the hierarchy between the PQ and the electroweak breaking scales remains radiatively stable thanks to the emergence of an extended Poincaré symmetry of the action [101, 102]. This is reflected by the fact that $\lambda_{1,2}^\phi \rightarrow 0$ and $\mu_\phi \rightarrow 0$ correspond to fixed points of the renormalization group evolution (see e.g. App. B in [103]).

To match with the more standard 2HDM notation (see e.g. [48]) we consider the rotated doublets

$$\begin{pmatrix} \Phi_1 \\ \Phi_2 \end{pmatrix} = \begin{pmatrix} c_\beta & s_\beta \\ -s_\beta & c_\beta \end{pmatrix} \begin{pmatrix} \tilde{H}_1 \\ \tilde{H}_2 \end{pmatrix}, \quad (\text{A.5})$$

so that Φ_1 picks up the whole electroweak VEV

$$\Phi_1 = \begin{pmatrix} G^+ \\ -\frac{1}{\sqrt{2}}(v + c_\beta h_1^0 + s_\beta h_2^0 - iG^0) \end{pmatrix}, \quad \Phi_2 = \begin{pmatrix} H^+ \\ -\frac{1}{\sqrt{2}}(-s_\beta h_1^0 + c_\beta h_2^0 - iA) \end{pmatrix}. \quad (\text{A.6})$$

Here we have defined the would-be Goldstone bosons

$$G^+ = c_\beta h_1^+ + s_\beta h_2^+, \quad G^0 = c_\beta \eta_1 + s_\beta \eta_2, \quad (\text{A.7})$$

and the scalar radial modes

$$H^+ = -s_\beta h_1^+ + c_\beta h_2^+, \quad A^0 = -s_\beta \eta_1 + c_\beta \eta_2. \quad (\text{A.8})$$

In the rotated basis the scalar potential reads

$$V(\Phi_1, \Phi_2) = M_{11}^2 \Phi_1^\dagger \Phi_1 + M_{22}^2 \Phi_2^\dagger \Phi_2 - \left(M_{12} \Phi_1^\dagger \Phi_2 + \text{h.c.} \right)$$

$$\begin{aligned}
& + \frac{\Lambda_1}{2}(\Phi_1^\dagger \Phi_1)^2 + \frac{\Lambda_2}{2}(\Phi_2^\dagger \Phi_2)^2 + \Lambda_3(\Phi_1^\dagger \Phi_1)(\Phi_2^\dagger \Phi_2) + \Lambda_4(\Phi_1^\dagger \Phi_2)(\Phi_2^\dagger \Phi_1) \\
& + \left\{ \frac{1}{2}\Lambda_5(\Phi_1^\dagger \Phi_2)^2 + \left[\Lambda_6(\Phi_1^\dagger \Phi_1) + \Lambda_7(\Phi_2^\dagger \Phi_2) \right] \Phi_1^\dagger \Phi_2 + \text{h.c.} \right\}, \tag{A.9}
\end{aligned}$$

with the new parameters given by

$$M_{11}^2 = m_{11}^2 c_\beta^2 + m_{22}^2 s_\beta^2 - \text{Re } m_{12}^2 s_{2\beta}, \tag{A.10}$$

$$M_{22}^2 = m_{11}^2 s_\beta^2 + m_{22}^2 c_\beta^2 - \text{Re } m_{12}^2 s_{2\beta}, \tag{A.11}$$

$$M_{12}^2 = \frac{1}{2} (m_{11}^2 - m_{22}^2) s_{2\beta} + \text{Re } m_{12}^2 c_{2\beta} + i \text{Im } m_{12}^2, \tag{A.12}$$

$$\Lambda_1 = \lambda_1 c_\beta^4 + \lambda_2 s_\beta^4 + \frac{1}{2}(\lambda_3 + \lambda_4) s_{2\beta}^2, \tag{A.13}$$

$$\Lambda_2 = \lambda_1 s_\beta^4 + \lambda_2 c_\beta^4 + \frac{1}{2}(\lambda_3 + \lambda_4) s_{2\beta}^2, \tag{A.14}$$

$$\Lambda_3 = \frac{1}{4} s_{2\beta}^2 [\lambda_1 + \lambda_2 - 2(\lambda_3 + \lambda_4)] + \lambda_3, \tag{A.15}$$

$$\Lambda_4 = \frac{1}{4} s_{2\beta}^2 [\lambda_1 + \lambda_2 - 2(\lambda_3 + \lambda_4)] + \lambda_4, \tag{A.16}$$

$$\Lambda_5 = \frac{1}{4} s_{2\beta}^2 [\lambda_1 + \lambda_2 - 2(\lambda_3 + \lambda_4)], \tag{A.17}$$

$$\Lambda_6 = -\frac{1}{2} s_{2\beta} [\lambda_1 c_\beta^2 - \lambda_2 s_\beta^2 - c_{2\beta}(\lambda_3 + \lambda_4)], \tag{A.18}$$

$$\Lambda_7 = -\frac{1}{2} s_{2\beta} [\lambda_1 s_\beta^2 - \lambda_2 c_\beta^2 + c_{2\beta}(\lambda_3 + \lambda_4)]. \tag{A.19}$$

The stationary conditions read

$$\left. \frac{\partial V}{\partial \Phi_1} \right|_{\langle \Phi_2 \rangle=0, \langle \Phi_1 \rangle=\frac{v}{\sqrt{2}}} = 0, \implies M_{11}^2 \frac{v}{\sqrt{2}} + \Lambda_1 \frac{v^3}{2\sqrt{2}} = 0, \tag{A.20}$$

$$\left. \frac{\partial V}{\partial \Phi_2} \right|_{\langle \Phi_2 \rangle=0, \langle \Phi_1 \rangle=\frac{v}{\sqrt{2}}} = 0, \implies -M_{12}^2 \frac{v}{\sqrt{2}} + \Lambda_6 \frac{v^3}{2\sqrt{2}} = 0, \tag{A.21}$$

from which we can substitute M_{11}^2 and M_{12}^2 into the scalar potential. The squared mass terms of the CP-odd and charged scalars can be read directly from the Lagrangian

$$m_{H^\pm}^2 = M_{22}^2 + \frac{1}{2} v^2 \Lambda_3, \tag{A.22}$$

$$m_A^2 = m_{H^\pm}^2 + \frac{1}{2} v^2 (\Lambda_4 - \Lambda_5) = M_{22}^2 + \frac{1}{2} v^2 (\Lambda_3 + \Lambda_4 - \Lambda_5), \tag{A.23}$$

while to obtain those of the CP-even Higgses we perform the rotation

$$\begin{pmatrix} h_2^0 \\ h_1^0 \end{pmatrix} = \begin{pmatrix} c_\alpha & s_\alpha \\ -s_\alpha & c_\alpha \end{pmatrix} \begin{pmatrix} h \\ H \end{pmatrix}. \tag{A.24}$$

This is equivalent to go into the basis where only one Higgs gets the whole electroweak VEV

$$\begin{pmatrix} m_H^2 & 0 \\ 0 & m_h^2 \end{pmatrix} = \begin{pmatrix} c_{\alpha-\beta} & s_{\alpha-\beta} \\ -s_{\alpha-\beta} & c_{\alpha-\beta} \end{pmatrix} \begin{pmatrix} \Lambda_1 v^2 & \Lambda_6 v^2 \\ \Lambda_6 v^2 & m_A^2 + \Lambda_5 v^2 \end{pmatrix} \begin{pmatrix} c_{\alpha-\beta} & -s_{\alpha-\beta} \\ s_{\alpha-\beta} & c_{\alpha-\beta} \end{pmatrix}, \tag{A.25}$$

with eigenvalues

$$m_{h,H}^2 = \frac{1}{2} \left(m_A^2 + v^2 (\Lambda_1 + \Lambda_5) \mp \sqrt{[m_A^2 + (\Lambda_5 - \Lambda_1) v^2]^2 + 4 v^4 \Lambda_6^2} \right), \tag{A.26}$$

and mixing angle given by [48]

$$s_{2(\alpha-\beta)} = \frac{2\Lambda_6 v^2}{m_H^2 - m_h^2}, \quad c_{2(\alpha-\beta)} = \frac{(\Lambda_1 - \Lambda_5)v^2 - m_A^2}{m_H^2 - m_h^2}. \quad (\text{A.27})$$

A useful quantity (appearing into Higgs couplings) is

$$c_{\alpha-\beta}^2 = \frac{\Lambda_1 v^2 - m_h^2}{m_H^2 - m_h^2} = \frac{\Lambda_6^2 v^4}{(m_H^2 - m_h^2)(m_H^2 - \Lambda_1 v^2)}, \quad (\text{A.28})$$

while some of the previous equations can be rearranged as

$$\Lambda_1 v^2 = m_h^2 s_{\alpha-\beta}^2 + m_H^2 c_{\alpha-\beta}^2, \quad (\text{A.29})$$

$$\Lambda_6 v^2 = (m_h^2 - m_H^2) s_{\alpha-\beta} c_{\alpha-\beta}, \quad (\text{A.30})$$

$$m_A^2 + \Lambda_5 v^2 = m_H^2 s_{\alpha-\beta}^2 + m_h^2 c_{\alpha-\beta}^2. \quad (\text{A.31})$$

Finally, Eq. (2.11) provides the embedding of the physical mass eigenstates in the original basis of the PQ-Higgs doublets.

Note that $s_{\alpha-\beta} = 0$ corresponds to $\Lambda_6 = 0$. In this scenario the field H is *aligned* to the electroweak VEV, making H to be SM-like with $m_H^2 = \Lambda_1 v^2$ [49]. In the opposite case where $c_{\alpha-\beta} = 0$ we have instead $m_h^2 = \Lambda_1 v^2$, corresponding to a SM-like h . This can be obtained by taking $m_H^2 \gg v^2$, which from Eq. (A.28) that corresponds to $c_{\alpha-\beta} \sim 1/m_H^2$. This scenario is called *alignment with decoupling* [50]. From Eq. (A.31) one also obtains

$$m_A^2 + \Lambda_5 v^2 \simeq m_H^2. \quad (\text{A.32})$$

Hence, in the decoupling scenario the scalar masses become degenerate, $m_H^2 \simeq m_A^2 \simeq m_{H^\pm}^2$. This is instead not the case for the alignment without decoupling, where the scalar masses remain at the electroweak scale and, in general, are non-degenerate. Such a case requires $\Lambda_6 \rightarrow 0$ and it can lead to a non-SM-like Higgs either above or below 125 GeV, see [49, 50] respectively.

B 4-fermion operators

We list here the 4-fermion operators which arise in Eq. (2.18), upon integrating out at tree level the radial modes of the PQ-2HDM. In the quark sector we obtain

$$\begin{aligned} \mathcal{L}_{\text{EFT}}^{4\text{-quark}} = & (C_{ijkl}^{\bar{u}_L u_R \bar{u}_L u_R} \bar{u}_{Li} u_{Rj} \bar{u}_{Lk} u_{Rl} + \text{h.c.}) + (C_{ijkl}^{\bar{d}_L d_R \bar{d}_L d_R} \bar{d}_{Li} d_{Rj} \bar{d}_{Lk} d_{Rl} + \text{h.c.}) \\ & + (C_{ijkl}^{\bar{u}_L u_R \bar{d}_L d_R} \bar{u}_{Li} u_{Rj} \bar{d}_{Lk} d_{Rl} + \text{h.c.}) + (C_{ijkl}^{\bar{u}_L u_R \bar{d}_R d_L} \bar{u}_{Li} u_{Rj} \bar{d}_{Rk} d_{Ll} + \text{h.c.}) \\ & + C_{ijkl}^{\bar{u}_L u_R \bar{u}_R u_L} \bar{u}_{Li} u_{Rj} \bar{u}_{Rk} u_{Ll} + C_{ijkl}^{\bar{d}_L d_R \bar{d}_R d_L} \bar{d}_{Li} d_{Rj} \bar{d}_{Rk} d_{Ll} \\ & + (C_{ijkl}^{\bar{u}_L d_R \bar{d}_L u_R} \bar{u}_{Li} d_{Rj} \bar{d}_{Lk} u_{Rl} + \text{h.c.}) + C_{ijkl}^{\bar{u}_L d_R \bar{d}_R u_L} \bar{u}_{Li} d_{Rj} \bar{d}_{Rk} u_{Ll} \\ & + C_{ijkl}^{\bar{d}_L u_R \bar{u}_R d_L} \bar{d}_{Li} u_{Rj} \bar{u}_{Rk} d_{Ll}, \end{aligned} \quad (\text{B.1})$$

where the 4-quark Wilson coefficients are found to be

$$C_{ijkl}^{\bar{u}_L u_R \bar{u}_L u_R} = \frac{1}{2m_H^2} C_{ij}^{H_u} C_{kl}^{H_u} + \frac{1}{2m_A^2} C_{ij}^{A_u} C_{kl}^{A_u} + \frac{1}{2m_h^2} C_{ij}^{h_u} C_{kl}^{h_u}, \quad (\text{B.2})$$

$$C_{ijkl}^{\bar{u}_L u_R \bar{d}_L d_R} = \frac{1}{2m_H^2} C_{ij}^{H_u} C_{kl}^{H_d} + \frac{1}{2m_A^2} C_{ij}^{A_u} C_{kl}^{A_d} + \frac{1}{2m_h^2} C_{ij}^{h_u} C_{kl}^{h_d}, \quad (\text{B.3})$$

$$C_{ijkl}^{\bar{d}_L d_R \bar{d}_L d_R} = \frac{1}{2m_H^2} C_{ij}^{H_d} C_{kl}^{H_d} + \frac{1}{2m_A^2} C_{ij}^{A_d} C_{kl}^{A_d} + \frac{1}{2m_h^2} C_{ij}^{h_d} C_{kl}^{h_d}, \quad (\text{B.4})$$

$$C_{ijkl}^{\bar{u}_L u_R \bar{d}_R d_L} = \frac{1}{2m_H^2} C_{ij}^{H_u} (C_{lk}^{H_d})^* + \frac{1}{2m_A^2} C_{ij}^{A_u} (C_{lk}^{A_d})^* + \frac{1}{2m_h^2} C_{ij}^{h_u} (C_{lk}^{h_d})^*, \quad (\text{B.5})$$

$$C_{ijkl}^{\bar{u}_L u_R \bar{u}_R u_L} = \frac{1}{m_H^2} C_{ij}^{H_u} (C_{lk}^{H_u})^* + \frac{1}{m_A^2} C_{ij}^{A_u} (C_{lk}^{A_u})^* + \frac{1}{m_h^2} C_{ij}^{h_u} (C_{lk}^{h_u})^*, \quad (\text{B.6})$$

$$C_{ijkl}^{\bar{d}_L d_R \bar{d}_R d_L} = \frac{1}{m_H^2} C_{ij}^{H_d} (C_{lk}^{H_d})^* + \frac{1}{m_A^2} C_{ij}^{A_d} (C_{lk}^{A_d})^* + \frac{1}{m_h^2} C_{ij}^{h_d} (C_{lk}^{h_d})^*, \quad (\text{B.7})$$

$$C_{ijkl}^{\bar{u}_L d_R \bar{d}_L u_R} = \frac{2}{m_{H^\pm}^2} V_{nj} V_{mk}^* C_{in}^{H_d^+} C_{ml}^{H_u^-}, \quad (\text{B.8})$$

$$C_{ijkl}^{\bar{u}_L d_R \bar{d}_R u_L} = \frac{2}{m_{H^\pm}^2} V_{nj} V_{mk}^* C_{in}^{H_d^+} (C_{lm}^{H_u^+})^*, \quad (\text{B.9})$$

$$C_{ijkl}^{\bar{d}_L u_R \bar{u}_R d_L} = \frac{2}{m_{H^\pm}^2} V_{ni}^* V_{ml} C_{nj}^{H_u^-} (C_{mk}^{H_u^-})^*. \quad (\text{B.10})$$

For the semi-leptonic operators we find

$$\begin{aligned} \mathcal{L}_{\text{EFT}}^{\text{semi-lept}} = & (C_{ijkl}^{\bar{q}_L q_R \bar{e}_L e_R} \bar{q}_{Li} q_{Rj} \bar{e}_{Lk} e_{Rl} + \text{h.c.}) + (C_{ijkl}^{\bar{q}_L q_R \bar{e}_R e_L} \bar{q}_{Li} q_{Rj} \bar{e}_{Rk} e_{Ll} + \text{h.c.}) \\ & + (C_{ijkl}^{\bar{\nu}_L e_R \bar{d}_R u_L} \bar{\nu}_{Li} e_{Rj} \bar{d}_{Rk} u_{Ll} + \text{h.c.}) + (C_{ijkl}^{\bar{\nu}_L e_R \bar{d}_R u_L} \bar{\nu}_{Li} e_{Rj} \bar{d}_{Rk} u_{Ll} + \text{h.c.}), \end{aligned} \quad (\text{B.11})$$

with Wilson coefficients

$$C_{ijkl}^{\bar{u}_L u_R \bar{e}_L e_R} = \frac{1}{m_H^2} C_{ij}^{H_u} C_{kl}^{H_e} + \frac{1}{m_A^2} C_{ij}^{A_u} C_{kl}^{A_e} + \frac{1}{m_h^2} C_{ij}^{h_u} C_{kl}^{h_e}, \quad (\text{B.12})$$

$$C_{ijkl}^{\bar{d}_L d_R \bar{e}_L e_R} = \frac{1}{m_H^2} C_{ij}^{H_d} C_{kl}^{H_e} + \frac{1}{m_A^2} C_{ij}^{A_d} C_{kl}^{A_e} + \frac{1}{m_h^2} C_{ij}^{h_d} C_{kl}^{h_e}, \quad (\text{B.13})$$

$$C_{ijkl}^{\bar{u}_L u_R \bar{e}_R e_L} = \frac{1}{m_H^2} C_{ij}^{H_u} (C_{lk}^{H_e})^* + \frac{1}{m_A^2} C_{ij}^{A_u} (C_{lk}^{A_e})^* + \frac{1}{m_h^2} C_{ij}^{h_u} (C_{lk}^{h_e})^*, \quad (\text{B.14})$$

$$C_{ijkl}^{\bar{d}_L d_R \bar{e}_R e_L} = \frac{1}{m_H^2} C_{ij}^{H_d} (C_{lk}^{H_e})^* + \frac{1}{m_A^2} C_{ij}^{A_d} (C_{lk}^{A_e})^* + \frac{1}{m_h^2} C_{ij}^{h_d} (C_{lk}^{h_e})^*, \quad (\text{B.15})$$

$$C_{ijkl}^{\bar{\nu}_L e_R \bar{d}_L u_R} = \frac{2}{m_{H^\pm}^2} U_{ni}^* V_{mk}^* C_{nj}^{H_e^+} C_{ml}^{H_u^-}, \quad (\text{B.16})$$

$$C_{ijkl}^{\bar{\nu}_L e_R \bar{d}_R u_L} = \frac{2}{m_{H^\pm}^2} U_{ni}^* V_{mk}^* C_{nj}^{H_e^+} (C_{lm}^{H_u^+})^*. \quad (\text{B.17})$$

Finally, the purely leptonic effective operators are

$$\begin{aligned} \mathcal{L}_{\text{EFT}}^{4\text{-lept}} = & (C_{ijkl}^{\bar{e}_L e_R \bar{e}_L e_R} \bar{e}_{Li} e_{Rj} \bar{e}_{Lk} e_{Rl} + \text{h.c.}) + C_{ijkl}^{\bar{e}_L e_R \bar{e}_R e_L} \bar{e}_{Li} e_{Rj} \bar{e}_{Rk} e_{Ll} \\ & + C_{ijkl}^{\bar{\nu}_L e_R \bar{e}_R \nu_L} \bar{\nu}_{Li} e_{Rj} \bar{e}_{Rk} \nu_{Ll}, \end{aligned} \quad (\text{B.18})$$

with Wilson coefficients

$$C_{ijkl}^{\bar{e}_L e_R \bar{e}_L e_R} = \frac{1}{2m_H^2} C_{ij}^{H_e} C_{kl}^{H_e} + \frac{1}{2m_A^2} C_{ij}^{A_e} C_{kl}^{A_e} + \frac{1}{2m_h^2} C_{ij}^{h_e} C_{kl}^{h_e}, \quad (\text{B.19})$$

$$C_{ijkl}^{\bar{e}_L e_R \bar{e}_R e_L} = \frac{1}{m_H^2} C_{ij}^{H_e} (C_{lk}^{H_e})^* + \frac{1}{m_A^2} C_{ij}^{A_e} (C_{lk}^{A_e})^* + \frac{1}{m_h^2} C_{ij}^{h_e} (C_{lk}^{h_e})^*, \quad (\text{B.20})$$

$$C_{ijkl}^{\bar{\nu}_L e_R \bar{e}_R \nu_L} = \frac{2}{m_{H^\pm}^2} U_{ni}^* U_{ml} C_{nj}^{H_e^+} (C_{mk}^{H_e^+})^*. \quad (\text{B.21})$$

C Meson mixing bounds

The neutral current 4-quark operators in Eq. (B.1) contribute to $\Delta F = 2$ transitions, which are constrained by meson mixing observables. The effective $\Delta F = 2$ Hamiltonian is given by

$$\mathcal{H}_{\text{eff}}^{\Delta F=2} = \sum_i^5 C_i Q_i + \sum_i^5 \tilde{C}_i \tilde{Q}_i, \quad (\text{C.1})$$

with

$$Q_1 = \bar{q}_L^\alpha \gamma^\mu q_L'^\alpha \bar{q}_L^\beta \gamma_\mu q_L'^\beta, \quad (\text{C.2})$$

$$Q_2 = \bar{q}_R^\alpha q_L'^\alpha \bar{q}_R^\beta q_L'^\beta, \quad (\text{C.3})$$

$$Q_3 = \bar{q}_R^\alpha q_L'^\beta \bar{q}_R^\beta q_L'^\alpha, \quad (\text{C.4})$$

$$Q_4 = \bar{q}_R^\alpha q_L'^\alpha \bar{q}_L^\beta q_R'^\beta, \quad (\text{C.5})$$

$$Q_5 = \bar{q}_R^\alpha q_L'^\beta \bar{q}_L^\beta q_R'^\alpha. \quad (\text{C.6})$$

Here, α and β are color indices, while q and q' refer to two different quark flavours in the mesonic system. In the 2HDM case, that is relevant for our analysis, only the operators Q_2 and Q_4 are generated at tree level. However, it is well-known that QCD running effects induce other operators, and give a sizable contribution to those already present. Running effects will be taken into account by using the analytic formulas provided in Refs. [79–81], respectively for K , B and D meson mixing. The master formula encoding the running of the Wilson coefficients is given by

$$C_r(\mu) = \sum_i \sum_s \left(b_i^{(r,s)} + \eta c_i^{(r,s)} \right) \eta^{a_i} C_i(M_H), \quad (\text{C.7})$$

where, a , b , c are so-called “magic numbers”, which depend on the process at hand and are taken from the above-mentioned references. The running of the strong coupling is taken care by the factor $\eta = \alpha_s(m_H)/\alpha_s(M_Z)$, where we take as an input $\alpha_s(M_Z)$ and compute the QCD running at 2-loops up to the scale of the heavy NP, m_H , by means of the code RunDec [104]. The low-energy scale μ is set to 2, 4.6 and 2.8 GeV respectively for the K , B and D meson systems, in order to match with the scale of the corresponding hadronic matrix elements. The numerical inputs for the meson mixing analysis are given in Table 3, where we defined the QCD running coefficients $\eta_i = C_i(\mu)/C_i(m_H)$ and $\eta_{ij} = C_i(\mu)/C_j(m_H)$, and we have taken as a reference value $m_H = 1$ TeV. Taking into account the renormalization group evolution of the Wilson coefficient for $\Delta F = 2$ transition, the meson mixing amplitudes read [79]

$$M_{ij} = \frac{\langle X | \mathcal{H}_{\text{eff}}^{\Delta F=2} | \bar{X} \rangle}{2M_X} = M_X f_X^2 \left[-\frac{5}{24} \frac{M_X^2}{(m_i^q + m_j^q)^2} \eta_2 B_2(\mu) ((C_2)_{ij} + (C_2^*)_{ji}) \right. \\ \left. + \left(\frac{1}{24} + \frac{1}{4} \frac{M_X^2}{(m_i^q + m_j^q)^2} \right) \eta_4 B_4(\mu) (C_4)_{ij} \right], \quad (\text{C.8})$$

where B_i are the so-called bag parameters which are calculated in lattice QCD (see Table 3 for the employed numerical values). Including also the contribution of NP, the meson-antimeson mass difference is given by (neglecting CP-violating phases)

$$\Delta m = 2|M_{12}^{\text{SM}} + M_{12}^{\text{NP}}|. \quad (\text{C.9})$$

	$K^0 - \bar{K}^0$	$B^0 - \bar{B}^0$	$B_s^0 - \bar{B}_s^0$	$D - \bar{D}$
$\Delta m [\text{GeV}] \times 10^{-15}$	3.484 ± 0.006	333.4 ± 1.3	11693 ± 8	6.7 ± 0.8
$M_M [\text{GeV}]$	0.497	5.279	5.367	1.864
$f_M [\text{GeV}]$	0.156	0.192	0.228	0.209
B_2	0.50	0.77	0.82	0.66
B_4	0.92	1.08	1.03	0.84
η_2	2.50	1.99	1.99	2.30
η_{32}	-1.70×10^{-3}	-0.024	-0.024	-0.013
η_4	4.78	3.10	3.10	3.97
η_{45}	0.18	0.086	0.086	0.14

Table 3: Numerical inputs for the analysis of $\Delta F = 2$ observables, including experimental values for meson-antimeson mass differences and meson masses [105], meson decay constants [83], bag parameters for $K^0 - \bar{K}^0$ [83], $B_d^0 - \bar{B}_d^0$ and $B_s^0 - \bar{B}_s^0$ [106], $D^0 - \bar{D}^0$ [107], as well as QCD running coefficients (see text).

Taking into account that the new physics contribution can be either positive or negative, and that the SM uncertainty is much larger than the experimental one (which is henceforth neglected), we conservatively consider the 2σ bounds:

$$\Delta m^{exp} = \Delta m^{\text{SM}} - 2\sigma_{\Delta m}^{\text{SM}} + 2|M_{12}^{\text{NP}}|, \quad \text{for } M_{12} > 0, \quad (\text{C.10})$$

$$\Delta m^{exp} = \Delta m^{\text{SM}} + 2\sigma_{\Delta m}^{\text{SM}} - 2|M_{12}^{\text{NP}}|, \quad \text{for } M_{12} < 0. \quad (\text{C.11})$$

Regarding theoretical predictions, for the $B_d^0 - \bar{B}_d^0$ and $B_s^0 - \bar{B}_s^0$ mixing we will employ the values $\Delta m_d = 3.51_{-0.24}^{+0.15} \times 10^{-13} \text{ GeV}$ and $\Delta m_s = 1.211_{-0.079}^{+0.046} \times 10^{-11} \text{ GeV}$ from Ref. [82], which are obtained by averaging lattice QCD and sum rules results. For $K^0 - \bar{K}^0$ mixing we take $\Delta m_K = (3.3 \pm 1.2) \times 10^{-15} \text{ GeV}$, that is the FLAG21 value [83] (see also [84]). For $D^0 - \bar{D}^0$ mixing a reliable SM prediction is still lacking, and hence we will just impose that new physics does not overshoot the experimental value at 2σ . Taking all of the above into account and applying Eqs. (C.10)–(C.11) we obtain

$$\left| -0.16 \left((C_2^d)_{12} + (C_2^d)_{21}^* \right) + 0.69 (C_4^d)_{12} \right| = [2.0, 2.5] \cdot 10^{-15} \text{ GeV}, \quad (\text{C.12})$$

$$\left| -0.20 \left((C_2^d)_{13} + (C_2^d)_{31}^* \right) + 0.57 (C_4^d)_{13} \right| = [4.6, 3.0] \cdot 10^{-14} \text{ GeV}, \quad (\text{C.13})$$

$$\left| -0.28 \left((C_2^d)_{23} + (C_2^d)_{32}^* \right) + 0.82 (C_4^d)_{23} \right| = [1.3, 1.2] \cdot 10^{-12} \text{ GeV}, \quad (\text{C.14})$$

where the number to the left is for the case in which the new physics contribution is negative, while the number on the right is for the case in which it is positive. For D mixing instead the bound reads

$$\left| -0.16 \left((C_2^u)_{12} + (C_2^u)_{21}^* \right) + 0.53 (C_4^u)_{12} \right| = 8.3 \cdot 10^{-15} \text{ GeV}. \quad (\text{C.15})$$

In this Appendix we have fixed as a reference the running of the $d(u)$ -type sector to 1(10) TeV, while in the numerical analysis in Section 3 we have properly taken into account running effects as a function of m_H . Note that employing model-independent constraints on individual Wilson coefficients would lead to an incorrect bound for the 2HDM case, since a specific combination of Wilson coefficients is actually constrained.

The operators associated to the Wilson coefficients C_2^f and C_4^f are obtained from Eq. (B.1), with the conditions $i = k$, $j = l$ and $i \neq j$. Using this information, one can rewrite the Wilson coefficients in terms of ϵ_{ij}^f as follows

$$C_2^d = \frac{(\epsilon_{ij}^d)^2}{4c_\beta^2} \left(\frac{m_A^2 - m_H^2}{m_H^2 m_A^2} + c_{\alpha-\beta}^2 \frac{m_H^2 - m_h^2}{m_H^2 m_h^2} \right), \quad (\text{C.16})$$

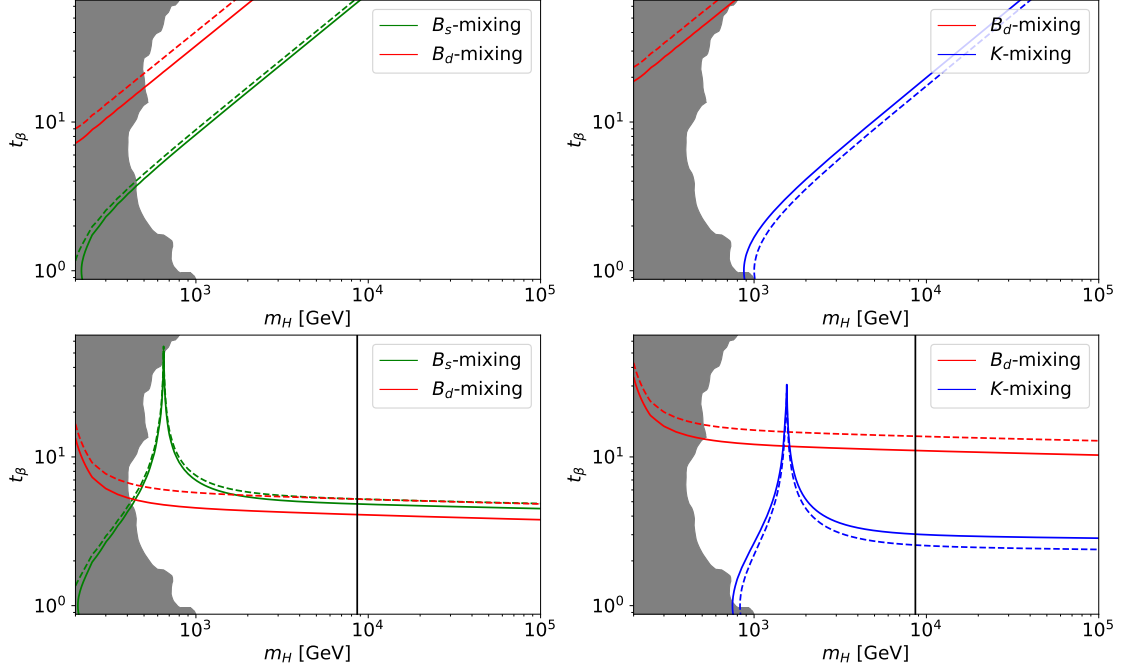


Figure 4: Left (right) panel plots show the meson mixing bounds for the M1 (M4) model, with the solid (dashed) line corresponding to a positive (negative) new physics contribution. The top panels correspond to $c_{\alpha-\beta} = 0$ and the bottom ones to $c_{\alpha-\beta} = 0.1$. The black vertical line in the bottom panels indicates the value of m_H for which the condition $c_{\alpha-\beta} = 0.1$ saturates the perturbativity of the Λ_1 parameter, i.e. $\Lambda_1 \simeq 4\pi$. LHC direct searches limits are displayed as well, taking as a reference those for the case of the type-II 2HDM (grey shaded region).

$$C_4^d = \frac{\epsilon_{ij}^d \epsilon_{ji}^{d*}}{2c_\beta^2} \left(\frac{m_A^2 + m_H^2}{m_H^2 m_A^2} + c_{\alpha-\beta}^2 \frac{m_H^2 - m_h^2}{m_H^2 m_h^2} \right), \quad (\text{C.17})$$

and similarly for the up-quark sector, which is obtained by replacing $c_\beta \rightarrow s_\beta$ in the above formulae. Since $c_{\alpha-\beta}$ is bounded by Higgs observables, the second term in Eqs. (C.16)–(C.17) is somewhat suppressed. In fact, this becomes obvious in the case of alignment, $c_{\alpha-\beta} \simeq 0$, with and without decoupling. In the alignment scenarios the Wilson coefficients can be further simplified as

$$C_2^f = 0, \quad C_4^f = \frac{\epsilon_{ij}^f \epsilon_{ji}^{f*}}{c_\beta^2 m_H^2}, \quad (\text{with decoupling}) \quad (\text{C.18})$$

$$C_2^f = \frac{\epsilon_{ij}^f}{4c_\beta^2} \frac{m_A^2 - m_H^2}{m_H^2 m_A^2}, \quad C_4^f = \frac{\epsilon_{ij}^f \epsilon_{ji}^{f*}}{2c_\beta^2} \frac{m_A^2 + m_H^2}{m_H^2 m_A^2}, \quad (\text{without decoupling}). \quad (\text{C.19})$$

Plugging in these expressions in Eqs. (C.12)–(C.15) and employing the definitions in Eqs. (2.28)–(2.29) it is straightforward to obtain the meson mixing bounds for the alignment scenarios, see Eqs. (3.1)–(3.4).

D Model-dependent bounds on the PQ-2HDM

In this Appendix we analyze other aspects of the PQ-2HDM which do not rely on the IR/UV connection discussed in this paper, but we assume a certain structure for the PQ charges and

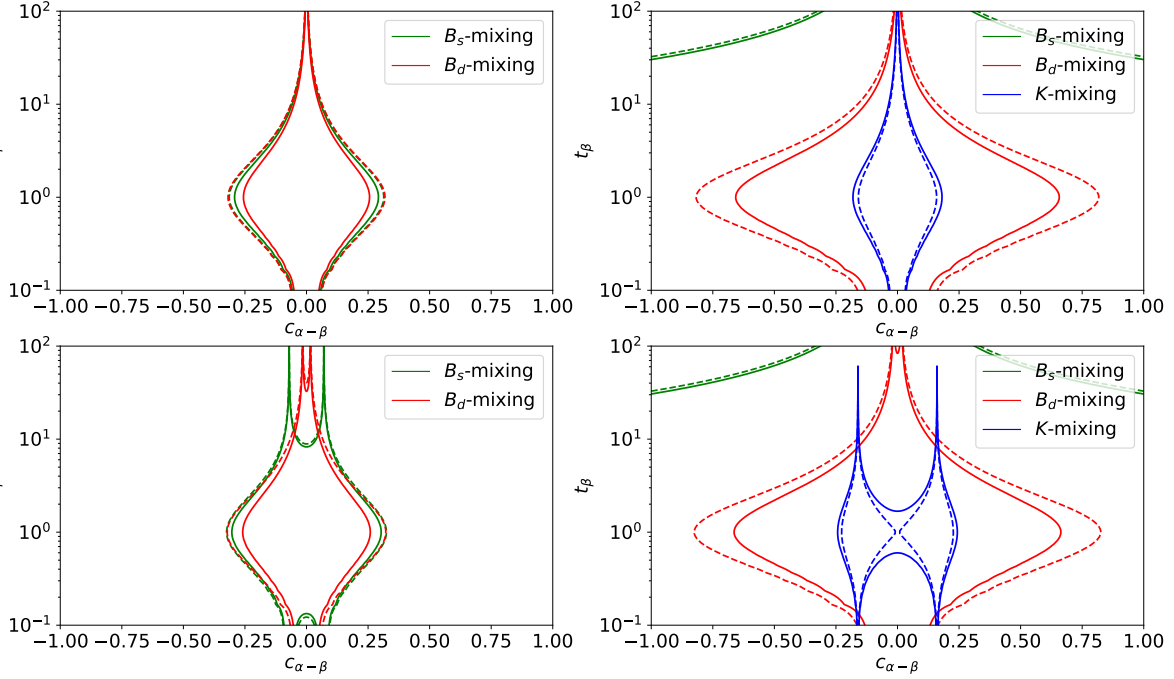


Figure 5: Left (right) panel plots show the meson mixing bounds due to the SM-like Higgs for the M1 (M4) model, with the solid (dashed) line corresponding to a positive (negative) new physics contribution. The top panels correspond to a decoupled m_H and the bottom ones to $m_H = 1$ TeV.

the mixing matrices. A possible ansatz is given for instance by $V_{d_{L,R}} = V_{\text{CKM}}$ and $V_{u_{L,R}} = \mathbf{1}$. Considering the M1 and M4 models introduced in Section 2, we can see from Fig. 4 that the bounds become much weaker once we introduce this CKM-like scenario. In the M1 model they are around 200 GeV. In fact, in this case the strongest bound does not come from K -mixing, since the PQ charge structure is such that an s - d transition is obtained after two CKM rotations of strength $\sim \lambda^3 \times \lambda^2$ and hence it is somewhat protected by the 2+1 structure of the PQ charges. In the M4 model instead, due to the PQ charge structure, the K -mixing leads to the strongest bound, being the s - d transition of order λ .

Note that in the meson mixing bounds (cf. Eqs. (3.1)–(3.4)) there could be a cancellation for $c_{\alpha-\beta} \neq 0$ (or $m_H \neq m_A$) which correspond to the bottom plots in Fig. 4. Hence, meson mixing does not rule out a relevant portion of the parameter space. For the M1 the model this is of the order of 200 GeV, while M4 is still in the reach of future LHC searches. Also, in the eventual discovery of a heavy Higgs, if we observe as well flavour mixing, the observed channel could help in reconstructing the flavour structure of the 2HDM.

For completeness, and for comparison with Ref. [37], we also show in Fig. 5 the meson mixing bounds in the $(c_{\alpha-\beta}, t_\beta)$ plane, for a fixed value of m_H . In particular, the top panel plots correspond to a mass parameter that is large enough to be considered in the decoupling regime, while the bottom ones are for $m_H = 1$ TeV. Here, we display the bound imposed by the SM-like Higgs component contributing to meson mixing. Note that it is not possible to decouple the heavier Higgs without sending to zero the mixing angle of the CP-even states. If we fix the mass of the second Higgs at 1 TeV, as in the bottom row of Fig. 5, then a possible cancellation in the meson mixing formula (cf. Eqs. (3.1)–(3.4)) is at play. This is an interesting parameter space region, since it can be potentially probed by Higgs flavour violating decays, such as $h \rightarrow bs$. As a final comment, we note that meson mixing constraints in the $(c_{\alpha-\beta}, t_\beta)$ plane are comparable to those obtained from lepton flavour violating observables (see e.g. [37]).

E Lepton flavour violating observables

In this Appendix we provide a compendium of formulae for LFV processes in the parametrization that allows us to make a direct connection between the IR and UV sources of flavour violation, including the leptonic decays $l_i \rightarrow 3l_j$, $l_i \rightarrow l_j l_k l_k$ and $l_i \rightarrow \gamma l_j$ as well as the LFV Higgs decays $h \rightarrow l_i l_j$. Employing the IR/UV relation in Eq. (2.24), the contribution of the heavy radial modes of the PQ-2HDM to the leptonic decays, $l_i \rightarrow 3l_j$, can be written as [87]

$$\text{BR}(l_i \rightarrow 3l_j) = \frac{m_\tau^5}{96\pi^3 \Gamma_\tau m_H^4} \left(\frac{m_j}{s_{2\beta} v} \right)^4 (C_e^A)_{jj}^2 \times \left[\left| (C_e^R)_{ji} + \frac{m_\tau}{m_j} (C_e^L)_{ji} \right|^2 + \left| (C_e^L)_{ji} + \frac{m_\tau}{m_e} (C_e^R)_{ji} \right|^2 \right], \quad (\text{E.1})$$

where we have neglected the mass of the final state lepton. This equation contains a combination of diagonal and off-diagonal components, thus making the IR/UV connection a bit more involved.⁶ Again, here we consider $f_a \gg m_H$, so that the direct axion contribution to this observable is negligible.

Within 2+1 PQ models (featuring axion flavour violation either in the LH or RH sector) the expression above gets further simplified into

$$\text{BR}(l_i \rightarrow 3l_j) = \frac{m_{f_i}^5}{96\pi^3 \Gamma_i m_H^4} \left(\frac{\sqrt{m_{f_j} m_{f_i}}}{s_{2\beta} v} \right)^4 (C_e^A)_{jj}^2 \left| (C_e^{R,L})_{ji} \right|^2. \quad (\text{E.2})$$

For $l_i \rightarrow l_j \bar{l}_k l_k$ decays we obtain instead (always in the case of 2+1 PQ models)

$$\begin{aligned} \text{BR}(l_i \rightarrow l_j \bar{l}_k l_k) &= \frac{m_{f_i}^5}{96\pi^3 \Gamma_i m_H^4} \left(\frac{m_{f_i}}{s_{2\beta} v} \right)^4 \left[(C_e^A)_{kk}^2 \left| (C_e^{R,L})_{ji} \right|^2 \frac{m_k^2}{m_i^2} \left(1 + \frac{m_j^2}{m_i^2} \right) \right. \\ &\quad \left. + \left| (C_e^{R,L})_{jk} \right|^2 \left| (C_e^{R,L})_{ki} \right|^2 \left(\frac{m_k^4}{m_i^4} + \frac{m_j^2}{m_i^2} \right) \right]. \end{aligned} \quad (\text{E.3})$$

Following [87] we can also write the one-loop contribution of the PQ-2HDM to the radiative LFV decays as

$$\text{BR}(l_i \rightarrow l_j \gamma) = \frac{m_{l_i}^5}{4\pi \Gamma_{l_i}} \left(|C_R^{l_j, l_i}|^2 + |C_L^{l_j, l_i}|^2 \right), \quad (\text{E.4})$$

in terms of the coefficients $C_{L(R)}^{l_j, l_i} = C_{L(R),+} + C_{L(R),0}$, denoting the sum of the charged and neutral contributions. For simplicity we will give them here for the case of 2+1 PQ models. The charged contribution reads

$$C_{R,+}^{l_j, l_i} = \frac{e}{384\pi^2 m_{H^\pm}^2} \left| C^{H_e^+} \right|_{ji}^2, \quad C_{L,+}^{l_j, l_i} = \frac{e}{384\pi^2 m_{H^\pm}^2} \frac{m_{l_j}}{m_{l_i}} \left| C^{H_e^+} \right|_{ji}^2, \quad (\text{E.5})$$

which we did not expand in terms of the axion couplings, since it includes both diagonal and off-diagonal couplings. The neutral contribution reads instead (working in the decoupling limit, $m_H^2 \simeq m_A^2$)

$$C_{L(R),0}^{l_j, l_i} = \frac{-e}{96\pi^2 m_H^2} \left(\frac{\sqrt{m_{e_i} m_{e_j}}}{v c_\beta s_\beta} \right)^2 \left[2(C_e^A)_{ii} (C_e^{L(R)})_{ji} + \left(1 + \frac{m_{e_j}^2}{m_{e_i}^2} \right) (C_e^A)_{jj} (C_e^{L(R)})_{ji} \right]$$

⁶In this case one could fix the diagonal axion coupling to electrons to the value suggested by the cooling hints [45], and then impose the LFV bounds in analogy to what done in Section 3.3 for the quark sector.

$$- \left(1 + \frac{m_{e_k}^2}{m_{e_i}^2} \right) (C_e^{L(R)})_{jk} (C_e^{L(R)})_{ik}^* \Big], \quad (\text{E.6})$$

$$C_{R(L),0}^{l_j,l_i} = \frac{e}{96\pi^2 m_H^2} \left(\frac{\sqrt{m_{e_i} m_{e_j}}}{v c_\beta s_\beta} \right)^2 \frac{m_{e_j}}{m_{e_i}} \left[2(C_e^A)_{jj} (C_e^{L(R)})_{ji} + \left(1 + \frac{m_{e_i}^2}{m_{e_j}^2} \right) (C_e^A)_{ii} (C_e^{L(R)})_{ji} \right. \\ \left. - \left(1 + \frac{m_{e_k}^2}{m_{e_j}^2} \right) (C_e^{L(R)})_{jk} (C_e^{L(R)})_{ik}^* \right], \quad (\text{E.7})$$

where $k \neq i, j$ is not summed over. Note that due to the structure of the loop contribution, it is not possible to obtain a straightforward connection with LFV axion observables. However, the bounds from radiative LFV decays such as $\mu \rightarrow e\gamma$ are very relevant for constraining the parameter space and they should be eventually taken into account in a global analysis.

We finally consider LFV Higgs decays, whose connection with LFV axion processes was discussed in Section 3.4. In this Appendix we provide full formulae, including the effects of a modified Higgs width and show that also flavour conserving Higgs decays can be related to axion physics. The complete formula for the LFV Higgs decays can be written as (in terms of LFV axion couplings, exploiting Eq. (2.24))

$$\text{BR}(h \rightarrow l_i l_j) = \frac{m_h}{16\pi\Gamma_h} \left(\frac{c_{\alpha-\beta}}{v s_\beta c_\beta} \right)^2 \left[\left(m_{l_i}^2 + m_{l_j}^2 \right) \left(|(C_e^L)_{ij}|^2 + |(C_e^R)_{ij}|^2 \right) \right. \\ \left. - 4m_{l_i} m_{l_j} \text{Re} \left((C_e^L)_{ij} (C_e^R)_{ij}^* \right) \right], \quad (\text{E.8})$$

where the Higgs width is modified as [37]

$$\Gamma_h \simeq \frac{k_h^2}{1 - B_h^{\text{BSM}}} \Gamma_{\text{SM}}, \quad (\text{E.9})$$

with B_h^{BSM} denoting the branching ratio of the beyond-the-SM contributions to the Higgs decay width, $\Gamma_h^{\text{SM}} \simeq 4.1 \text{ MeV}$ and k_h^2 parametrizing the effect due to Higgs couplings modifications. The latter is defined as [37]

$$k_h^2 \simeq 0.58k_b^2 + 0.22k_W^2 + 0.08k_g^2 + 0.06k_\tau^2 + 0.03k_c^2 + 0.03k_e^2 + 2.3 \times 10^{-3}k_\gamma^2 \\ + 1.5 \times 10^{-3}k_{Z\gamma}^2 + 4 \times 10^{-4}k_s^2 + 2.2 \times 10^{-4}k_\mu^2, \quad (\text{E.10})$$

in terms of the k -parameters

$$k_{f_i} \equiv \frac{\sqrt{2}m_f}{v} C_{ii}^{h_f} = -s_{\alpha-\beta} + \frac{c_{\alpha-\beta}}{c_\beta s_\beta} (C_f^A)_{ii}, \quad (\text{E.11})$$

where in the last step we have exploited again Eq. (2.24). In particular, the modified Higgs interactions with gauge couplings read

$$k_W = k_Z = s_{\alpha-\beta}, \quad (\text{E.12})$$

$$k_{Z\gamma}^2 \simeq 0.00348k_t^2 + 1.121k_W^2 - 0.1249k_t k_W, \quad (\text{E.13})$$

$$k_g^2 \simeq 1.04k_t^2 + 0.002k_b^2 - 0.04k_b k_t, \quad (\text{E.14})$$

$$k_\gamma^2 \simeq 1.59k_W^2 + 0.07k_t^2 - 0.67k_W k_t. \quad (\text{E.15})$$

Hence, the above expressions show that deviations in Higgs couplings can also be related to diagonal axion couplings.

References

- [1] R. D. Peccei and H. R. Quinn, “CP Conservation in the Presence of Instantons,” *Phys. Rev. Lett.* **38** (1977) 1440–1443.
- [2] R. D. Peccei and H. R. Quinn, “Constraints Imposed by CP Conservation in the Presence of Instantons,” *Phys. Rev.* **D16** (1977) 1791–1797.
- [3] S. Weinberg, “A New Light Boson?,” *Phys. Rev. Lett.* **40** (1978) 223–226.
- [4] F. Wilczek, “Problem of Strong p and t Invariance in the Presence of Instantons,” *Phys. Rev. Lett.* **40** (1978) 279–282.
- [5] M. Dine and W. Fischler, “The Not So Harmless Axion,” *Phys. Lett. B* **120** (1983) 137–141.
- [6] L. Abbott and P. Sikivie, “A Cosmological Bound on the Invisible Axion,” *Phys. Lett. B* **120** (1983) 133–136.
- [7] J. Preskill, M. B. Wise, and F. Wilczek, “Cosmology of the Invisible Axion,” *Phys. Lett. B* **120** (1983) 127–132.
- [8] A. R. Zhitnitsky, “On Possible Suppression of the Axion Hadron Interactions. (In Russian),” *Sov. J. Nucl. Phys.* **31** (1980) 260. [*Yad. Fiz.* 31,497(1980)].
- [9] M. Dine, W. Fischler, and M. Srednicki, “A Simple Solution to the Strong CP Problem with a Harmless Axion,” *Phys. Lett.* **B104** (1981) 199–202.
- [10] J. E. Kim, “Weak Interaction Singlet and Strong CP Invariance,” *Phys. Rev. Lett.* **43** (1979) 103.
- [11] M. A. Shifman, A. I. Vainshtein, and V. I. Zakharov, “Can Confinement Ensure Natural CP Invariance of Strong Interactions?,” *Nucl. Phys.* **B166** (1980) 493.
- [12] R. D. Peccei, T. T. Wu, and T. Yanagida, “A Viable Axion Model,” *Phys. Lett. B* **172** (1986) 435–440.
- [13] L. M. Krauss and F. Wilczek, “A Shortlived Axion Variant,” *Phys. Lett. B* **173** (1986) 189–192.
- [14] L. M. Krauss and D. J. Nash, “A Viable Weak Interaction Axion?,” *Phys. Lett. B* **202** (1988) 560–567.
- [15] M. Clemente, E. Berdermann, P. Kienle, H. Tsertos, W. Wagner, C. Kozhuharov, F. Bosch, and W. König, “Narrow positron lines from U - U and U - Th collisions,” *Phys. Lett. B* **137** (1984) 41–46.
- [16] J. Schweppe *et al.*, “Observation of a peak structure in positron spectra from U + Cm collisions,” *Phys. Rev. Lett.* **51** (1983) 2261–2264.
- [17] Y. Ema, K. Hamaguchi, T. Moroi, and K. Nakayama, “Flaxion: a minimal extension to solve puzzles in the standard model,” *JHEP* **01** (2017) 096, [arXiv:1612.05492 \[hep-ph\]](#).
- [18] L. Calibbi, F. Goertz, D. Redigolo, R. Ziegler, and J. Zupan, “Minimal axion model from flavor,” *Phys. Rev. D* **95** no. 9, (2017) 095009, [arXiv:1612.08040 \[hep-ph\]](#).
- [19] F. Arias-Aragon and L. Merlo, “The Minimal Flavour Violating Axion,” *JHEP* **10** (2017) 168, [arXiv:1709.07039 \[hep-ph\]](#). [Erratum: *JHEP* 11, 152 (2019)].
- [20] F. Björkeröth, L. Di Luzio, F. Mescia, and E. Nardi, “ $U(1)$ flavour symmetries as Peccei-Quinn symmetries,” *JHEP* **02** (2019) 133, [arXiv:1811.09637 \[hep-ph\]](#).
- [21] L. Di Luzio, F. Mescia, E. Nardi, P. Panci, and R. Ziegler, “Astrophobic Axions,” *Phys. Rev. Lett.* **120** no. 26, (2018) 261803, [arXiv:1712.04940 \[hep-ph\]](#).
- [22] F. Björkeröth, L. Di Luzio, F. Mescia, E. Nardi, P. Panci, and R. Ziegler, “Axion-electron decoupling in nucleophobic axion models,” *Phys. Rev. D* **101** no. 3, (2020) 035027, [arXiv:1907.06575 \[hep-ph\]](#).

- [23] L. Darmé, L. Di Luzio, M. Giannotti, and E. Nardi, “Selective enhancement of the QCD axion couplings,” *Phys. Rev. D* **103** no. 1, (2021) 015034, [arXiv:2010.15846 \[hep-ph\]](#).
- [24] L. Di Luzio, F. Mescia, E. Nardi, and S. Okawa, “Renormalization group effects in astrophobic axion models,” *Phys. Rev. D* **106** no. 5, (2022) 055016, [arXiv:2205.15326 \[hep-ph\]](#).
- [25] M. Badziak and K. Harigaya, “Naturally astrophobic QCD axion,” [arXiv:2301.09647 \[hep-ph\]](#).
- [26] F. Takahashi and W. Yin, “Hadrophobic Axion from GUT,” [arXiv:2301.10757 \[hep-ph\]](#).
- [27] C. Cornella, P. Paradisi, and O. Sumensari, “Hunting for ALPs with Lepton Flavor Violation,” *JHEP* **01** (2020) 158, [arXiv:1911.06279 \[hep-ph\]](#).
- [28] J. Martin Camalich, M. Pospelov, P. N. H. Vuong, R. Ziegler, and J. Zupan, “Quark Flavor Phenomenology of the QCD Axion,” *Phys. Rev. D* **102** no. 1, (2020) 015023, [arXiv:2002.04623 \[hep-ph\]](#).
- [29] L. Calibbi, D. Redigolo, R. Ziegler, and J. Zupan, “Looking forward to lepton-flavor-violating ALPs,” *JHEP* **09** (2021) 173, [arXiv:2006.04795 \[hep-ph\]](#).
- [30] M. Bauer, M. Neubert, S. Renner, M. Schnubel, and A. Thamm, “Flavor probes of axion-like particles,” *JHEP* **09** (2022) 056, [arXiv:2110.10698 \[hep-ph\]](#).
- [31] A. W. M. Guerrero and S. Rigolin, “Revisiting $K \rightarrow \pi a$ decays,” *Eur. Phys. J. C* **82** no. 3, (2022) 192, [arXiv:2106.05910 \[hep-ph\]](#).
- [32] J. A. Gallo, A. W. M. Guerrero, S. Peñaranda, and S. Rigolin, “Leptonic meson decays into invisible ALP,” *Nucl. Phys. B* **979** (2022) 115791, [arXiv:2111.02536 \[hep-ph\]](#).
- [33] Y. Jho, S. Knapen, and D. Redigolo, “Lepton-flavor violating axions at MEG II,” *JHEP* **10** (2022) 029, [arXiv:2203.11222 \[hep-ph\]](#).
- [34] A. W. M. Guerrero and S. Rigolin, “ALP production in weak mesonic decays,” *Fortsch. Phys.* **2023** (11, 2022) 2200192, [arXiv:2211.08343 \[hep-ph\]](#).
- [35] I. G. Irastorza and J. Redondo, “New experimental approaches in the search for axion-like particles,” *Prog. Part. Nucl. Phys.* **102** (2018) 89–159, [arXiv:1801.08127 \[hep-ph\]](#).
- [36] P. Sikivie, “Invisible Axion Search Methods,” *Rev. Mod. Phys.* **93** no. 1, (2021) 015004, [arXiv:2003.02206 \[hep-ph\]](#).
- [37] M. Badziak, G. Grilli di Cortona, M. Tabet, and R. Ziegler, “Flavor-violating Higgs decays and stellar cooling anomalies in axion models,” *JHEP* **10** (2021) 181, [arXiv:2107.09708 \[hep-ph\]](#).
- [38] L. Di Luzio, M. Giannotti, E. Nardi, and L. Visinelli, “The landscape of QCD axion models,” *Phys. Rept.* **870** (2020) 1–117, [arXiv:2003.01100 \[hep-ph\]](#).
- [39] L. Di Luzio, F. Mescia, and E. Nardi, “Redefining the Axion Window,” *Phys. Rev. Lett.* **118** no. 3, (2017) 031801, [arXiv:1610.07593 \[hep-ph\]](#).
- [40] L. Di Luzio, F. Mescia, and E. Nardi, “Window for preferred axion models,” *Phys. Rev. D* **96** no. 7, (2017) 075003, [arXiv:1705.05370 \[hep-ph\]](#).
- [41] K. Choi, S. H. Im, C. B. Park, and S. Yun, “Minimal Flavor Violation with Axion-like Particles,” *JHEP* **11** (2017) 070, [arXiv:1708.00021 \[hep-ph\]](#).
- [42] M. Chala, G. Guedes, M. Ramos, and J. Santiago, “Running in the ALPs,” *Eur. Phys. J. C* **81** no. 2, (2021) 181, [arXiv:2012.09017 \[hep-ph\]](#).
- [43] M. Bauer, M. Neubert, S. Renner, M. Schnubel, and A. Thamm, “The Low-Energy Effective Theory of Axions and ALPs,” *JHEP* **04** (2021) 063, [arXiv:2012.12272 \[hep-ph\]](#).

- [44] K. Choi, S. H. Im, H. J. Kim, and H. Seong, “Precision axion physics with running axion couplings,” *JHEP* **08** (2021) 058, [arXiv:2106.05816 \[hep-ph\]](#).
- [45] L. Di Luzio, M. Fedele, M. Giannotti, F. Mescia, and E. Nardi, “Stellar evolution confronts axion models,” *JCAP* **02** (2022) 035, [arXiv:2109.10368 \[hep-ph\]](#).
- [46] **ATLAS** Collaboration, “Combined measurements of Higgs boson production and decay using up to 139 fb^{-1} of proton-proton collision data at $\sqrt{s} = 13\text{ TeV}$ collected with the ATLAS experiment,”.
- [47] L. J. Hall and M. B. Wise, “Flavor Changing Higgs Boson Couplings,” *Nucl. Phys. B* **187** (1981) 397–408.
- [48] J. F. Gunion and H. E. Haber, “The CP conserving two Higgs doublet model: The Approach to the decoupling limit,” *Phys. Rev. D* **67** (2003) 075019, [arXiv:hep-ph/0207010](#).
- [49] J. Bernon, J. F. Gunion, H. E. Haber, Y. Jiang, and S. Kraml, “Scrutinizing the alignment limit in two-Higgs-doublet models: $m_h=125\text{ GeV}$,” *Phys. Rev. D* **92** no. 7, (2015) 075004, [arXiv:1507.00933 \[hep-ph\]](#).
- [50] J. Bernon, J. F. Gunion, H. E. Haber, Y. Jiang, and S. Kraml, “Scrutinizing the alignment limit in two-Higgs-doublet models. II. $m_H=125\text{ GeV}$,” *Phys. Rev. D* **93** no. 3, (2016) 035027, [arXiv:1511.03682 \[hep-ph\]](#).
- [51] **ATLAS** Collaboration, M. Aaboud *et al.*, “Search for additional heavy neutral Higgs and gauge bosons in the ditau final state produced in 36 fb^{-1} of pp collisions at $\sqrt{s} = 13\text{ TeV}$ with the ATLAS detector,” *JHEP* **01** (2018) 055, [arXiv:1709.07242 \[hep-ex\]](#).
- [52] **ATLAS** Collaboration, M. Aaboud *et al.*, “Search for WW/WZ resonance production in $\ell\nu qq$ final states in pp collisions at $\sqrt{s} = 13\text{ TeV}$ with the ATLAS detector,” *JHEP* **03** (2018) 042, [arXiv:1710.07235 \[hep-ex\]](#).
- [53] **ATLAS** Collaboration, M. Aaboud *et al.*, “Searches for heavy ZZ and ZW resonances in the $\ell\ell qq$ and $\nu\nu qq$ final states in pp collisions at $\sqrt{s} = 13\text{ TeV}$ with the ATLAS detector,” *JHEP* **03** (2018) 009, [arXiv:1708.09638 \[hep-ex\]](#).
- [54] **ATLAS** Collaboration, M. Aaboud *et al.*, “Search for heavy ZZ resonances in the $\ell^+\ell^-\ell^+\ell^-$ and $\ell^+\ell^-\nu\bar{\nu}$ final states using proton–proton collisions at $\sqrt{s} = 13\text{ TeV}$ with the ATLAS detector,” *Eur. Phys. J. C* **78** no. 4, (2018) 293, [arXiv:1712.06386 \[hep-ex\]](#).
- [55] **ATLAS** Collaboration, M. Aaboud *et al.*, “Search for heavy resonances decaying into WW in the $e\nu\mu\nu$ final state in pp collisions at $\sqrt{s} = 13\text{ TeV}$ with the ATLAS detector,” *Eur. Phys. J. C* **78** no. 1, (2018) 24, [arXiv:1710.01123 \[hep-ex\]](#).
- [56] **ATLAS** Collaboration, M. Aaboud *et al.*, “Search for heavy resonances decaying into a W or Z boson and a Higgs boson in final states with leptons and b -jets in 36 fb^{-1} of $\sqrt{s} = 13\text{ TeV}$ pp collisions with the ATLAS detector,” *JHEP* **03** (2018) 174, [arXiv:1712.06518 \[hep-ex\]](#). [Erratum: JHEP 11, 051 (2018)].
- [57] **ATLAS** Collaboration, M. Aaboud *et al.*, “Search for a heavy Higgs boson decaying into a Z boson and another heavy Higgs boson in the $\ell\ell bb$ final state in pp collisions at $\sqrt{s} = 13\text{ TeV}$ with the ATLAS detector,” *Phys. Lett. B* **783** (2018) 392–414, [arXiv:1804.01126 \[hep-ex\]](#).
- [58] **ATLAS** Collaboration, G. Aad *et al.*, “Reconstruction and identification of boosted di- τ systems in a search for Higgs boson pairs using 13 TeV proton-proton collision data in ATLAS,” *JHEP* **11** (2020) 163, [arXiv:2007.14811 \[hep-ex\]](#).
- [59] **ATLAS** Collaboration, G. Aad *et al.*, “Search for heavy resonances decaying into a pair of Z bosons in the $\ell^+\ell^-\ell'^+\ell'^-$ and $\ell^+\ell^-\nu\bar{\nu}$ final states using 139 fb^{-1} of proton–proton collisions at $\sqrt{s} = 13\text{ TeV}$ with the ATLAS detector,” *Eur. Phys. J. C* **81** no. 4, (2021) 332, [arXiv:2009.14791 \[hep-ex\]](#).

- [60] **ATLAS** Collaboration, G. Aad *et al.*, “Search for heavy Higgs bosons decaying into two tau leptons with the ATLAS detector using pp collisions at $\sqrt{s} = 13$ TeV,” *Phys. Rev. Lett.* **125** no. 5, (2020) 051801, [arXiv:2002.12223 \[hep-ex\]](#).
- [61] **CMS** Collaboration, A. M. Sirunyan *et al.*, “Search for a massive resonance decaying to a pair of Higgs bosons in the four b quark final state in proton-proton collisions at $\sqrt{s} = 13$ TeV,” *Phys. Lett. B* **781** (2018) 244–269, [arXiv:1710.04960 \[hep-ex\]](#).
- [62] **CMS** Collaboration, A. M. Sirunyan *et al.*, “Search for Higgs boson pair production in events with two bottom quarks and two tau leptons in proton–proton collisions at $\sqrt{s} = 13$ TeV,” *Phys. Lett. B* **778** (2018) 101–127, [arXiv:1707.02909 \[hep-ex\]](#).
- [63] **CMS** Collaboration, A. M. Sirunyan *et al.*, “Combination of searches for Higgs boson pair production in proton-proton collisions at $\sqrt{s} = 13$ TeV,” *Phys. Rev. Lett.* **122** no. 12, (2019) 121803, [arXiv:1811.09689 \[hep-ex\]](#).
- [64] **CMS** Collaboration, A. M. Sirunyan *et al.*, “Search for a heavy Higgs boson decaying to a pair of W bosons in proton-proton collisions at $\sqrt{s} = 13$ TeV,” *JHEP* **03** (2020) 034, [arXiv:1912.01594 \[hep-ex\]](#).
- [65] **CMS** Collaboration, A. M. Sirunyan *et al.*, “Search for a heavy pseudoscalar Higgs boson decaying into a 125 GeV Higgs boson and a Z boson in final states with two tau and two light leptons at $\sqrt{s} = 13$ TeV,” *JHEP* **03** (2020) 065, [arXiv:1910.11634 \[hep-ex\]](#).
- [66] **CMS** Collaboration, A. M. Sirunyan *et al.*, “Search for new neutral Higgs bosons through the $H \rightarrow ZA \rightarrow \ell^+ \ell^- b \bar{b}$ process in pp collisions at $\sqrt{s} = 13$ TeV,” *JHEP* **03** (2020) 055, [arXiv:1911.03781 \[hep-ex\]](#).
- [67] **CMS** Collaboration, A. M. Sirunyan *et al.*, “Search for heavy Higgs bosons decaying to a top quark pair in proton-proton collisions at $\sqrt{s} = 13$ TeV,” *JHEP* **04** (2020) 171, [arXiv:1908.01115 \[hep-ex\]](#). [Erratum: *JHEP* **03**, 187 (2022)].
- [68] **CMS** Collaboration, A. M. Sirunyan *et al.*, “Search for a heavy pseudoscalar boson decaying to a Z and a Higgs boson at $\sqrt{s} = 13$ TeV,” *Eur. Phys. J. C* **79** no. 7, (2019) 564, [arXiv:1903.00941 \[hep-ex\]](#).
- [69] **CMS** Collaboration, A. M. Sirunyan *et al.*, “Search for resonant pair production of Higgs bosons in the $bbZZ$ channel in proton-proton collisions at $\sqrt{s} = 13$ TeV,” *Phys. Rev. D* **102** no. 3, (2020) 032003, [arXiv:2006.06391 \[hep-ex\]](#).
- [70] **ATLAS** Collaboration, G. Aad *et al.*, “Search for dijet resonances in events with an isolated charged lepton using $\sqrt{s} = 13$ TeV proton-proton collision data collected by the ATLAS detector,” *JHEP* **06** (2020) 151, [arXiv:2002.11325 \[hep-ex\]](#).
- [71] **ATLAS** Collaboration, G. Aad *et al.*, “Search for charged Higgs bosons decaying into a top quark and a bottom quark at $\sqrt{s} = 13$ TeV with the ATLAS detector,” *JHEP* **06** (2021) 145, [arXiv:2102.10076 \[hep-ex\]](#).
- [72] **CMS** Collaboration, A. M. Sirunyan *et al.*, “Search for charged Higgs bosons in the $H^\pm \rightarrow \tau^\pm \nu_\tau$ decay channel in proton-proton collisions at $\sqrt{s} = 13$ TeV,” *JHEP* **07** (2019) 142, [arXiv:1903.04560 \[hep-ex\]](#).
- [73] **CMS** Collaboration, A. M. Sirunyan *et al.*, “Search for physics beyond the standard model in multilepton final states in proton-proton collisions at $\sqrt{s} = 13$ TeV,” *JHEP* **03** (2020) 051, [arXiv:1911.04968 \[hep-ex\]](#).
- [74] L. Wang, J. M. Yang, and Y. Zhang, “Two-Higgs-doublet models in light of current experiments: a brief review,” *Commun. Theor. Phys.* **74** no. 9, (2022) 097202, [arXiv:2203.07244 \[hep-ph\]](#).
- [75] O. Atkinson, M. Black, A. Lenz, A. Rusov, and J. Wynne, “Cornering the Two Higgs Doublet Model Type II,” *JHEP* **04** (2022) 172, [arXiv:2107.05650 \[hep-ph\]](#).

- [76] O. Atkinson, M. Black, C. Englert, A. Lenz, A. Rusov, and J. Wynne, “The flavourful present and future of 2HDMs at the collider energy frontier,” *JHEP* **11** (2022) 139, [arXiv:2202.08807 \[hep-ph\]](#).
- [77] K. S. Babu and S. Jana, “Enhanced Di-Higgs Production in the Two Higgs Doublet Model,” *JHEP* **02** (2019) 193, [arXiv:1812.11943 \[hep-ph\]](#).
- [78] T. P. Cheng and M. Sher, “Mass Matrix Ansatz and Flavor Nonconservation in Models with Multiple Higgs Doublets,” *Phys. Rev. D* **35** (1987) 3484.
- [79] M. Ciuchini *et al.*, “Delta M(K) and epsilon(K) in SUSY at the next-to-leading order,” *JHEP* **10** (1998) 008, [arXiv:hep-ph/9808328](#).
- [80] D. Becirevic, M. Ciuchini, E. Franco, V. Gimenez, G. Martinelli, A. Masiero, M. Papinutto, J. Reyes, and L. Silvestrini, “ $B_d - \bar{B}_d$ mixing and the $B_d \rightarrow J/\psi K_s$ asymmetry in general SUSY models,” *Nucl. Phys. B* **634** (2002) 105–119, [arXiv:hep-ph/0112303](#).
- [81] **UTfit** Collaboration, M. Bona *et al.*, “Model-independent constraints on $\Delta F = 2$ operators and the scale of new physics,” *JHEP* **03** (2008) 049, [arXiv:0707.0636 \[hep-ph\]](#).
- [82] L. Di Luzio, M. Kirk, A. Lenz, and T. Rauh, “ ΔM_s theory precision confronts flavour anomalies,” *JHEP* **12** (2019) 009, [arXiv:1909.11087 \[hep-ph\]](#).
- [83] **Flavour Lattice Averaging Group (FLAG)** Collaboration, Y. Aoki *et al.*, “FLAG Review 2021,” *Eur. Phys. J. C* **82** no. 10, (2022) 869, [arXiv:2111.09849 \[hep-lat\]](#).
- [84] J. Brod and M. Gorbahn, “Next-to-Next-to-Leading-Order Charm-Quark Contribution to the CP Violation Parameter ϵ_K and ΔM_K ,” *Phys. Rev. Lett.* **108** (2012) 121801, [arXiv:1108.2036 \[hep-ph\]](#).
- [85] G. C. Branco, W. Grimus, and L. Lavoura, “Relating the scalar flavor changing neutral couplings to the CKM matrix,” *Phys. Lett. B* **380** (1996) 119–126, [arXiv:hep-ph/9601383](#).
- [86] G. C. Branco, P. M. Ferreira, L. Lavoura, M. N. Rebelo, M. Sher, and J. P. Silva, “Theory and phenomenology of two-Higgs-doublet models,” *Phys. Rept.* **516** (2012) 1–102, [arXiv:1106.0034 \[hep-ph\]](#).
- [87] A. Crivellin, A. Kokulu, and C. Greub, “Flavor-phenomenology of two-Higgs-doublet models with generic Yukawa structure,” *Phys. Rev. D* **87** no. 9, (2013) 094031, [arXiv:1303.5877 \[hep-ph\]](#).
- [88] A. Crivellin, S. Najjari, and J. Rosiek, “Lepton Flavor Violation in the Standard Model with general Dimension-Six Operators,” *JHEP* **04** (2014) 167, [arXiv:1312.0634 \[hep-ph\]](#).
- [89] **BaBar** Collaboration, B. Aubert *et al.*, “Searches for Lepton Flavor Violation in the Decays $\tau^+ \rightarrow e^+ \gamma$ and $\tau^+ \rightarrow \mu^+ \gamma$,” *Phys. Rev. Lett.* **104** (2010) 021802, [arXiv:0908.2381 \[hep-ex\]](#).
- [90] **MEG** Collaboration, J. Adam *et al.*, “New constraint on the existence of the $\mu^+ \rightarrow e^+ \gamma$ decay,” *Phys. Rev. Lett.* **110** (2013) 201801, [arXiv:1303.0754 \[hep-ex\]](#).
- [91] **MEG** Collaboration, A. M. Baldini *et al.*, “Search for the lepton flavour violating decay $\mu^+ \rightarrow e^+ \gamma$ with the full dataset of the MEG experiment,” *Eur. Phys. J. C* **76** no. 8, (2016) 434, [arXiv:1605.05081 \[hep-ex\]](#).
- [92] **Belle** Collaboration, A. Abdesselam *et al.*, “Search for lepton-flavor-violating tau-lepton decays to $\ell \gamma$ at Belle,” *JHEP* **10** (2021) 19, [arXiv:2103.12994 \[hep-ex\]](#).
- [93] **SINDRUM** Collaboration, U. Bellgardt *et al.*, “Search for the Decay $\mu^+ \rightarrow e^+ e^- e^-$,” *Nucl. Phys. B* **299** (1988) 1–6.
- [94] K. Hayasaka *et al.*, “Search for Lepton Flavor Violating Tau Decays into Three Leptons with 719 Million Produced Tau+Tau- Pairs,” *Phys. Lett. B* **687** (2010) 139–143, [arXiv:1001.3221 \[hep-ex\]](#).

- [95] **CMS** Collaboration, A. M. Sirunyan *et al.*, “Search for lepton-flavor violating decays of the Higgs boson in the $\mu\tau$ and $e\tau$ final states in proton-proton collisions at $\sqrt{s} = 13$ TeV,” *Phys. Rev. D* **104** no. 3, (2021) 032013, [arXiv:2105.03007 \[hep-ex\]](#).
- [96] **ATLAS** Collaboration, “Searches for lepton-flavour-violating decays of the Higgs boson into $e\tau$ and $\mu\tau$ in $\sqrt{s} = 13$ TeV pp collisions with the ATLAS detector,” [arXiv:2302.05225 \[hep-ex\]](#).
- [97] R. Harnik, J. Kopp, and J. Zupan, “Flavor Violating Higgs Decays,” *JHEP* **03** (2013) 026, [arXiv:1209.1397 \[hep-ph\]](#).
- [98] **Belle-II** Collaboration, I. Adachi *et al.*, “Search for lepton-flavor-violating τ decays to a lepton and an invisible boson at Belle II,” [arXiv:2212.03634 \[hep-ex\]](#).
- [99] S. Bertolini, L. Di Luzio, H. Kolečová, and M. Malinský, “Massive neutrinos and invisible axion minimally connected,” *Phys. Rev. D* **91** no. 5, (2015) 055014, [arXiv:1412.7105 \[hep-ph\]](#).
- [100] D. Espriu, F. Mescia, and A. Renau, “Axion-Higgs interplay in the two Higgs-doublet model,” *Phys. Rev. D* **92** no. 9, (2015) 095013, [arXiv:1503.02953 \[hep-ph\]](#).
- [101] R. R. Volkas, A. J. Davies, and G. C. Joshi, “Naturalness of the Invisible Axion Model,” *Phys. Lett. B* **215** (1988) 133–138.
- [102] R. Foot, A. Kobakhidze, K. L. McDonald, and R. R. Volkas, “Poincaré protection for a natural electroweak scale,” *Phys. Rev. D* **89** no. 11, (2014) 115018, [arXiv:1310.0223 \[hep-ph\]](#).
- [103] S. Bertolini, L. Di Luzio, H. Kolečová, M. Malinský, and J. C. Vasquez, “Neutrino-axion-dilaton interconnection,” *Phys. Rev. D* **93** no. 1, (2016) 015009, [arXiv:1510.03668 \[hep-ph\]](#).
- [104] F. Herren and M. Steinhauser, “Version 3 of RunDec and CRunDec,” *Comput. Phys. Commun.* **224** (2018) 333–345, [arXiv:1703.03751 \[hep-ph\]](#).
- [105] **Particle Data Group** Collaboration, P. A. Zyla *et al.*, “Review of Particle Physics,” *PTEP* **2020** no. 8, (2020) 083C01.
- [106] R. J. Dowdall, C. T. H. Davies, R. R. Horgan, G. P. Lepage, C. J. Monahan, J. Shigemitsu, and M. Wingate, “Neutral B-meson mixing from full lattice QCD at the physical point,” *Phys. Rev. D* **100** no. 9, (2019) 094508, [arXiv:1907.01025 \[hep-lat\]](#).
- [107] N. Carrasco *et al.*, “ $D^0 - \bar{D}^0$ mixing in the standard model and beyond from $N_f = 2$ twisted mass QCD,” *Phys. Rev. D* **90** no. 1, (2014) 014502, [arXiv:1403.7302 \[hep-lat\]](#).